

# Can Robotic Cues Manipulate Human Decisions? Exploring Consensus Building via Bias-Controlled Non-linear Opinion Dynamics and Robotic Eye Gaze Mediated Interaction in Human-Robot Teaming

RAJUL KUMAR, Department of Electrical and Computer Engineering, George Mason University, USA

ADAM BHATTI, Department of Electrical and Computer Engineering, George Mason University, USA

NINGSHI YAO\*, Department of Electrical and Computer Engineering, George Mason University, USA

Although robots are becoming more advanced with human-like anthropomorphic features and decision-making abilities to improve collaboration, the active integration of humans into this process remains under-explored. This article presents the first experimental study exploring decision-making interactions between humans and robots with visual cues from robotic eyes, which can dynamically influence human opinion formation. The cues generated by robotic eyes gradually guide human decisions towards alignment with the robot's choices. Both human and robot decision-making processes are modeled as non-linear opinion dynamics with evolving biases. To examine these opinion dynamics under varying biases, we conduct numerical parametric and equilibrium continuation analyses using tuned parameters designed explicitly for the presented human-robot interaction experiment. Furthermore, to facilitate the transition from disagreement to agreement, we introduced a human opinion observation algorithm integrated with the formation of the robot's opinion, where the robot's behavior is controlled based on its formed opinion. The algorithms developed aim to enhance human involvement in consensus building, fostering effective collaboration between humans and robots. Experiments with 51 participants ( $N = 51$ ) show that human-robot teamwork can be improved by guiding human decisions using robotic cues. Finally, we provide detailed insights on the effects of trust, cognitive load, and participant demographics on decision-making based on user feedback and post-experiment interviews.

CCS Concepts: • **Human-centered computing** → **HCI theory, concepts and models**.

Additional Key Words and Phrases: Human-Robot Teaming, Consensus, Bias in Human-Robot Interaction, Human-in-loop, External Stimulus, Non-Linear Opinion Dynamics, Robotics Eye Gaze

## ACM Reference Format:

Rajul Kumar, Adam Bhatti, and Ningshi Yao. 2018. Can Robotic Cues Manipulate Human Decisions? Exploring Consensus Building via Bias-Controlled Non-linear Opinion Dynamics and Robotic Eye Gaze Mediated Interaction in Human-Robot Teaming. In *Proceedings of ACM Trans. Hum.-Robot Interact.*. ACM, New York, NY, USA, 35 pages. <https://doi.org/XXXXXXX.XXXXXXX>

---

This research was partially supported by NSF Grant ECCS-2218517. It was approved by the Institutional Review Board (IRB [2125317-1]) and the Office of Research Integrity and Assurance at George Mason University, Fairfax, Virginia, USA..

Authors' Contact Information: Rajul Kumar, rkumar29@gmu.edu, Department of Electrical and Computer Engineering, George Mason University, Fairfax, Virginia, USA; Adam Bhatti, abhatti@potomacschool.org, Department of Electrical and Computer Engineering, George Mason University, Fairfax, Virginia. The author contributed to this work as part of the Aspiring Scientists Summer Internship Program (ASSIP) 2024 at George Mason University. His primary affiliation is with The Potomac School in McLean, Virginia, USA; Ningshi Yao, nyao4@gmu.edu, Department of Electrical and Computer Engineering, George Mason University, Fairfax, Virginia, USA.

---

Permission to make digital or hard copies of all or part of this work for personal or classroom use is granted without fee provided that copies are not made or distributed for profit or commercial advantage and that copies bear this notice and the full citation on the first page. Copyrights for components of this work owned by others than the author(s) must be honored. Abstracting with credit is permitted. To copy otherwise, or republish, to post on servers or to redistribute to lists, requires prior specific permission and/or a fee. Request permissions from [permissions@acm.org](mailto:permissions@acm.org).

© 2018 Copyright held by the owner/author(s). Publication rights licensed to ACM.

Manuscript submitted to ACM

Manuscript submitted to ACM

## 1 INTRODUCTION

In recent years, the lack of safe and efficient human-robot collaboration in industrial environments has promoted negative perceptions of robots among human workers, substantially preventing the adoption of robotic technologies [59, 66]. As depicted in Figure 1, robots are still restricted to safety cages, reinforcing the physical segregation between robots and human-operated work spaces. Even in routine industrial assembly tasks, critical thinking and decision-making are often required, emphasizing the need for human oversight and collaboration, as robots alone are insufficient [44]. While robots excel at repetitive tasks, humans are better suited for decision-making in uncertain conditions, necessitating mutual collaboration and co-learning between humans and robots. These insights highlight the need for safe human-robot collaboration to optimize industrial operations and the urgent need for new research into efficient, secure interactions.

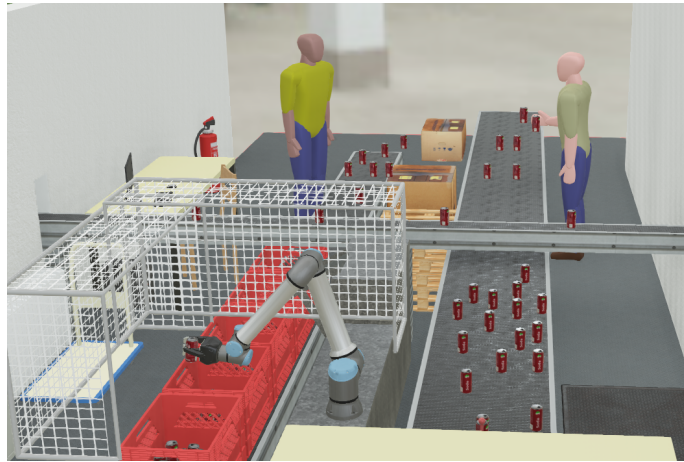


Fig. 1. Problem-motivation example illustrating the real-world challenge of robotic arms operating in safety cages within a can packaging warehouse, highlighting the lack of direct human-robot collaboration and the separation of workspace.

The existing literature often overlooks the crucial role of human contribution in human-robot teaming, instead focusing on outsmarting or handling uncertainties in human actions, which are often considered partially known information. As a result, robot control behavior is frequently designed using techniques such as partially observable Markov decision processes (or POMDPs), predictive model control, or reinforcement learning. However, human behavior is inherently unpredictable and mainly irrational [27]. In the absence of strategic guidance or communication toward a collaborative decision, human participants can engage in behaviors that trick, test, or attempt to surpass the capabilities of their robotic counterparts. In recent work, robots regulate human behavior using haptic feedback systems [19] and a combination of visual cues and haptic wristbands [20] to communicate intentions of movement, prompting workers to adjust their actions, thereby preventing collisions. However, the scalability of this approach is limited in complex industrial environments with frequent human-robot interactions, and it may struggle with highly dynamic tasks where trajectories and actions are constantly changing. In [8], the robot regulates human behavior through expressive facial expressions, body posture, and vocal signals to convey its effective state. This creates a feedback loop where the human adjusts their decisions based on the robot's cues, resulting in synchronization of body language and effective alignment. A key limitation here is the difficulty of sustaining nuanced human-robot interactions over longer

durations in unpredictable environments, where emotional synchronization becomes more challenging. Furthermore, the limited anthropomorphic characteristics of the robot can reduce its overall expressive capability. A more detailed examination of robot communication and clues to humans, specifically through robotic eyes, is provided in Subsections 2.2 and 2.4 of Section 2.

The process by which human opinions are formed during interactions is a crucial aspect of human-robot collaboration. Robotic cues and communication strategies must be dynamically generated and evolve in response to these opinions. Since human opinion formation is highly non-linear and influenced by various psychological factors that are not yet fully understood, integrating these factors, such as continuously evolving biases and opinions, into robot behavior presents a significant challenge. Balancing robot autonomy with human control in interactive scenarios is equally complex. Given the diversity of human behavior and the variability in individual beliefs, robot opinions must dynamically adapt to human responses and uncertainties in real time, making tuning the parameters of the decision-making model both critical and complex. Moreover, developing robots that can guide human decisions through cues while simultaneously exhibiting anthropomorphic traits and human-like decision-making abilities introduces additional complexities. This requires a robust theoretical understanding of how opinions shaped by robotic cues, acting as external stimuli, lead to agreement or disagreement under a given set of parameters for human and robot mental models, as well as the conditions that give rise to these outcomes.

Incorporating humans into robotic decision-making is crucial and fosters nuanced interactions, where humans not only provide real-time feedback but also adapt their strategies based on the robot's guidance, enhancing learning for both. In ethically sensitive areas such as healthcare, integrating human oversight in robotic decision-making is important and not only ensures that moral considerations guide outcomes but also enhance trust and safety. By maintaining human control, especially in high-stakes environments, we can provide a crucial fail-safe against potential robotic errors, ensuring that decisions reflect ethical reasoning and mitigate risks effectively.

Motivated by these challenges and the identified research gap in guiding human behavior during interactions with robots, as well as the numerous benefits of human involvement in human-robot collaboration, this research investigates the following key research questions.

- a) **RQ1:** Can bias or external stimulus be deliberately imparted to human decision making as a psychological factor to effectively achieve consensus with robot during interaction?
- b) **RQ2:** If assimilated, how do humans perceive and react to biases conveyed through robotic eye cues in terms of trust, persuasion, and collaboration?
- c) **RQ3:** Does persistent disagreement in early interactions motivate humans to subsequently align their choices with those of robots when mediated by visual cues as external biasing factor?
- d) **RQ4:** Under a chosen specified set of parameters, can non-linear opinion dynamics, representing both human and robot mental models, with and without bias control, accurately model real-time robot decisions and achieve controlled consensus or dissensus in response to human actions?
- e) **RQ5:** Can the robotic eye design presented in this paper serve as an effective anthropomorphic mechanism to guide humans toward a specific collaborative choice with the robot?

To establish a foundation for investigating these questions, we first iteratively refined the non-linear opinion dynamics parameters through trial and error, for the experimental settings outlined in Section 3. Under the chosen optimized parameters, we demonstrate how bias can be used as a control parameter in a two-agent, two-choice non-linear opinion system to facilitate a transition from repeated disagreement to agreement. Through numerical parametric and equilibrium continuation analysis, we identified the critical bias settings that enable the transition to both consensus

and dissensus. Then, to facilitate consensus between humans and robots, whose opinions evolve dynamically during interactions, we introduced a Bias Control Algorithm that continuously adjusts robot and human biases to align with the collaborative convergence choice of both agents.

Through the development of a choice-based decision-making experiment involving a human and a robotic arm, acting as either cooperative or competitive agents, we explored research questions (RQ1-RQ5). The robot was proactively controlled using a behavior control algorithm, and we demonstrated how real-time human opinions can be observed and manipulated through visual cues from a robotic eye as a bias during interactions. The rest of this article is organized as follows: Section 2 provides a comprehensive review of both past and recent related work, delineating the specific contributions this article makes to the field. Section 3 details the experimental setup, including component design and the procedural methodology. Section 4 presents the bias parametric analysis for the selected non-linear dynamics parameter set, along with the proposed opinion formation and robot behavior algorithms. Section 5 presents the incorporation of human into co-learning interactions with the robot, through the use of robotic eye gaze. The subsequent sections 6, 7, and 8 present experimental demonstrations, insights from user feedback analysis, and concluding remarks, respectively.

## 2 RELATED WORK and CONTRIBUTIONS

In this section, we outline the related work and our contributions to human-robot teaming, emphasizing the application of non-linear opinion dynamics, experimental design, and human-in-the-loop considerations during interactions.

### 2.1 Human Mental Models and Opinion Dynamics

Humans can inherently predict others' behavior using internal mental models [12]. Despite extensive literature on human decision-making frameworks [22], this domain continues to present unresolved challenges. Historically, theories such as risk-based prospect theory [28] and dual-process theory [29] have been proposed, with drift-diffusion models (DDMs) for binary decision-making scenarios [24, 47]. A recent study using DDMs to model human drivers decision-making in left-turn scenarios highlighted key flaws: while DDMs predict outcomes, they fail to account for the impact of time-to-arrival on response times [62], highlighting the need for more comprehensive human behavioral models. Later, the theory of mind (TOM), encompassing false beliefs, intentions, and desires, gained prominence [49].

Theory of Mind (TOM) requires an understanding of unspoken social norms and emotional subtleties, often communicated through symbolic language, which is challenging to implement in robots lacking human-like cognitive structures [15, 51, 58]. Research by [11] explores the implementation of TOM through visual cues, yet it remains limited to specific scenarios like obstacle avoidance and robot-robot interactions. To date, no comprehensive mathematical model for applying Theory of Mind to robots exists, highlighting significant limitations for its use in human-robot interactions [45]. Cognitively akin to TOM, Bayesian models [14, 31], often integrated with TOM [3, 21], model human decision-making (excluding human-robot interaction). Although they provide clear mathematical traceability, these models fail to account for individual variability and heavily depend on initial human beliefs, which can vary widely. Moreover, their computationally intensive belief updates by integration of new evidence and recalculation of posterior probabilities, limits their applicability in real-time human-robot interactions.

Very recently, breakthroughs in deep learning [17], reinforcement learning [54], spiking neural networks [40], and quantum reinforcement learning [36] have emerged in human decision-making research. However, these methods demand extensive training data or can experience sample inefficiency, challenging to address in human-robot interactions and currently addressed by sim-to-real techniques. Additionally, the black-box nature of reinforcement learning complicates hyper-parameter tuning due to its lack of mathematical traceability. Both Bayesian and reinforcement

learning (RL) techniques extend the Rescorla-Wagner model [48], addressing some of its limitations [18]. Although applicable to human intent prediction [61], the Rescorla-Wagner model has key shortcomings, such as excluding cognitive processes such as memory, bias, attention, and relying on a static conditioned stimulus [39].

In this research, we developed a new dynamic model for updating bias in non-linear opinion dynamics, specifically tailored for human-robot interaction with a tuned parameter set. The employed non-linear opinion dynamics model effectively captures the temporal evolution of multi-agent opinion formation processes [5, 35]. As noted by [33], non-linear models are more effective because human decision-making processes themselves are inherently non-linear. In human-robot interactions, this model can enable rapid and computationally efficient collective decision making while incorporating psychological factors such as memory, bias, social influence, and attention. In addition, it offers strong mathematical traceability, facilitating controlled hyper-parameter tuning.

## 2.2 Robot Control in Human-Robot Teaming

Effective human-robot collaboration relies on trust built through robots' safe and proactive decision-making. Much of the existing literature uses Markov Decision Processes (MDPs) [53, 55] and Partially Observable Markov Decision Processes (POMDPs) [38, 60] to control robot behavior. Although MDPs and POMDPs are robust in managing uncertainty, they do not typically account for individual differences, and their reliance on abstract environmental features that are non-intuitive to humans, which can make the robot's behavior seem unpredictable. In contrast, opinion dynamics explicitly incorporates observable social and psychological factors into robot actions and models other agents' actions as opinions, considering individual variability, thereby enhancing predictability and trust. It improves robotic intuitiveness and dynamically adapts to human responses and perceived needs, which are crucial to building consensus between humans and robots.

The first application of non-linear opinion dynamics for robot navigation control, presented in [10] to address collision avoidance in confrontational human-robot navigation, presents an innovative yet unilateral approach. This approach disproportionately assigns all collaborative navigation responsibilities to the robot, positioning it as the only active participant in collaborative efforts and marginalizing human involvement. Moreover, in instances where persistent disagreements occur within non-linear opinion dynamics, Section V.C in [5] explores the transition from disagreement to agreement by dynamically modulating the inter-agent coupling weight of influence on the same opinion. However, should scenarios arise where persistent disagreements lead to continuous collisions, the concept of inter-agent coupling weight—defined as the robot's influence on a human's heading decisions—proves impractical for transitioning from disagreement to agreement. Directly measuring and applying inter-agent coupling weight as a control input for consensus building in real-world scenarios is challenging. In contrast, biases or external stimuli, which are comparatively easier to measure, can be effectively imparted to humans through visual cues like eye gaze towards a specific option, providing a feasible alternative [42].

To the best of the authors' knowledge, this is the first study to incorporate bias or external stimuli into robot actions, exploring collaborative outcomes by influencing human opinions with bias, thereby making the collaborative process bidirectional in building consensus.

## 2.3 Experimental Design in Human-Robot Collaborative Learning

To validate robot control algorithms and human mental models, researchers have designed various experimental frameworks that simulate real world scenarios. The study in [57] details an experiment in which humans and robots are tasked with placing tiles in color-matched slots. However, this study, along with [23], restricts the variability of decisions

during a trial, failing to capture the nuanced complexity of real-world interactions. Furthermore, [34] introduces a Collaborative Cup Stacking Task where neither humans shift their strategies from less to more stable cup stacking configurations during a trial, nor do robots guide them to enhance performance, impacting the task's optimal outcome.

Despite extensive research on intelligent decision-making models, many experimental frameworks delegate only strategic decision-making tasks to humans, relegating robots to logistical roles such as retrieving and supplying assembly parts [13]. This does not fully leverage robot capabilities, leading to the under-utilization of their potential in collaborative tasks. In contrast, the study by [37] demonstrates humans performing agile tasks using VR technology, while robots manage hazardous operations, coordinated via a mutual cognitive system. However, the broad application of these methods is limited by the impracticality of using specialized VR (Virtual Reality) devices in everyday industrial settings.

But our experimental setup, designed to simulate complex real-world scenarios, maximizes the predictive and proactive capabilities of both humans and robots. Human participants can change their preferences during the trial, and the robot adapts in real-time to human decisions by taking controlled actions. This approach focuses on analyzing human decision-making strategies, rather than merely having humans perform a joint task with robots. Moreover, our experiment incorporates external psychological factors such as cognitive load, external bias, and performance motivation. The dynamic interaction model, in which the robot initially disagrees before seeking agreement, simulates complex human social behaviors, distinguishing it from past experiments designed for controlled static interactions.

## 2.4 Human-in-loop and Robotics Cues

For rapid and reliable consensus building between humans and robots, it is essential to incorporate a human-in-the-loop co-learning process. This involves not only integrating human actions into the robot's decision-making but also allowing humans to actively contribute to collaborative efforts. A recent study [50] demonstrates that human opinions can be influenced through strategic interactions with robots. Studies have explored verbal communication, where robots answer human queries [46] and humans respond to robot queries [30], facilitating mutual understanding and consensus building for optimal task completion. Furthermore, [55] found that bidirectional verbal and non-verbal communication enhances human-robot task efficiency through dynamic information exchange. Beyond verbal interaction, non-verbal cues, such as visual communication, offer a quick, effective, and natural way to express intentions. [64] and [32] show that humans spontaneously adopt a robot's visual perspective, especially when the robot exhibits anthropomorphic characteristics, though the study does not delve into decision-making scenarios from the robot's side.

Robotic eye gaze has been shown to serve as an effective predictive cue during interactions; however, existing studies are predominantly limited to screen-based eye gaze experiments [42]. Additionally, other research suggests that real 3D robotic interactions are more effective and differ markedly from on-screen interactions [52]. Building on this insight, researchers have focused on the development of realistic robotic eyes and their interactions within physical environments [9]. For instance, an anthropomorphic humanoid robot using scripted eye gaze behaviors in the Chicken game was employed; however, these behaviors were neither dynamically adaptive nor based on any decision-making mental model, which limited real-time interaction [4]. Similarly, studies have investigated whether robots could utilize human eye gaze to enhance collaboration, but the focus was on task completion with prescribed robot responses and lacked repeated decision-making, as well as a mathematically traceable or data-driven mental model [7].

In our human-robot experimental setup, we provided a detailed explanation of the functionality of the realistic robotic eye used to deliver visual cues that bias human decisions. By leveraging robotic eye gaze, the robot can non-verbally influence human behavior, effectively mimicking human social cues and enhancing the naturalness and intuitiveness

of interactions. This method significantly improves collaboration, promoting smoother and more socially integrated inclusion of robots in human teams. Considering the identified gaps and shortcomings in the literature, the main contributions of this paper are summarized as follows.

1. We present a novel experimental study on imparting bias to human opinions and integrating them into a co-learning loop with the robot, facilitating significant human contributions to consensus building. Robot’s decisions are modeled and controlled using bias-adjusted nonlinear opinion dynamics.
2. We introduce the first application of dynamic bias in non-linear opinion dynamics for consensus building, using anthropomorphic robotic eye gaze as a biasing mechanism. Furthermore, we investigate the correlation between the increase in visual cues from the robotic eye and the corresponding increase in human trust over time.
3. For the presented human-robot interaction scenario, we tuned the parameter set of the non-linear opinion dynamics. For this tuned parameter set, we developed a dynamic model of bias and performed a parametric analysis to describe the system’s behavior under varying bias conditions. Through continuation analysis of the unique opinion equilibrium, we elucidate the mechanisms driving the robot’s transition to consensus, particularly how dynamic self-biasing predominates when surpassing the maximum potential impact of collective social influence from human opinions on the robot.
4. Our pioneering experiment establishes a strategic bi-directional decision-making process between humans and robots, characterized by a tightly integrated co-learning closed loop. Initially, we examine the impact of the robot’s repeated disagreement on human decision-making and collaboration outcomes. Furthermore, we investigate whether this initial disagreement motivates humans to align their decisions with robotic visual cues in subsequent iterations.
5. Our experimental investigations, involving a diverse cohort of human participants, revealed their perceptions of robotic eye cues and initial robot opinion disagreements. By conducting comprehensive user feedback analysis, we elucidate new findings on human trust dynamics concerning anthropomorphic robotic eye-based visual cues, aimed at facilitating consensus building.

### 3 METHOD : EXPERIMENTAL SETUP, COMPONENTS and PROCEDURE

We designed a controlled yet realistic experimental framework, as detailed in Subsection 3.1. In this human-robot interaction experiment, mutual cooperation between the human participant and the robot is essential to achieve the designated game objective. During the game, the actions of both agents are modeled as opinions that vary non-linearly over time. The individual hardware and software components utilized in the experiment, such as the robotic eye and vision-based opinion tracking, are elaborated upon in further detail in Subsections 3.1.1 and 3.1.2, respectively.

#### 3.1 Experimental Setup and Components

In the experimental setup depicted in Figure 2(a) and 2(b), separate sets of buzzers, each comprising a red and a blue buzzer, are designated for human and robot to press, capturing their steady-state opinion choices at the end of each trial. These buzzers are strategically positioned to maximize visibility, ensuring easy identification of each agent’s choices, and allowing both agents to face each other while maintaining a safe distance. We used a 6-DOF collaborative Ned2 robotic arm [1] as the robotic counterpart of human participants. Throughout the experiment, each participant’s performance is continuously evaluated on the basis of their choices during each decision-making trial with the robot.

The current scores of the participants are continuously displayed on a nearby screen to motivate them to effectively collaborate with the robot. Additionally, once participants cross the marked black line—referred to as the ‘decision commit line’ in Figure 2(a)—they are instructed not to change their opinions, ensuring consistency in steady-state

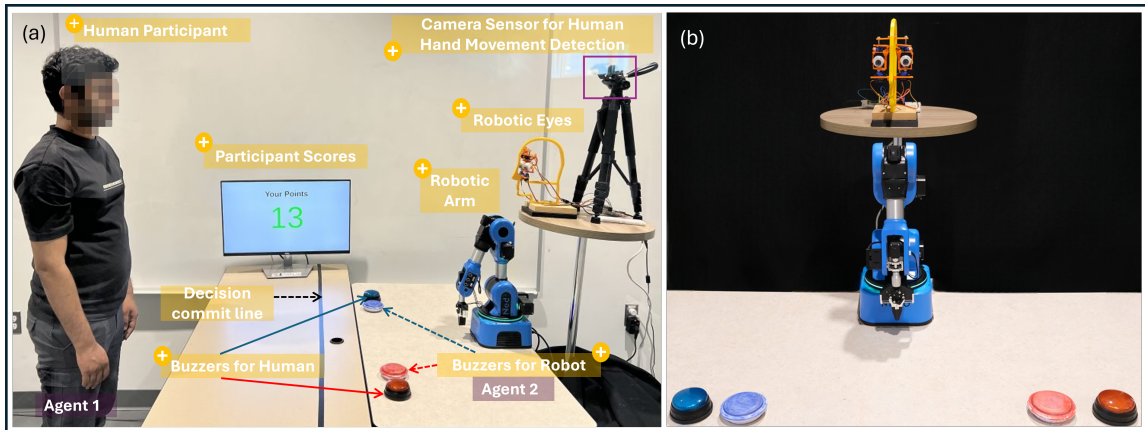


Fig. 2. (a) Experimental setup for a two-agent, two-choice decision-making task between a human and a robot (with human consent obtained for image use and identity disclosure). The setup includes red and blue buzzers for the human to press, red and blue puck lights buzzers for the robot, a robotic eye, a camera sensor, and a screen that continuously displays the participant’s score. (b) The right figure illustrates the view from the participant’s perspective, showing the robotic arm counterpart and the robotic eye.

decision-making and safety. To steer human participants’ opinions toward consensus, a robotic eye was strategically positioned on a separate circular table, elevated and situated behind the robotic arm, ensuring a clear and direct line of sight for the human participants. A speaker, programmed to emit the auditory cue ‘1, 2, 3, go,’ was positioned behind the robotic eye and connected to a central control station, allowing synchronized execution of the robotic arm, eyes, and camera sensors. Additionally, to observe both transient and steady-state human opinions during decision-making, a high-resolution overhead camera focused on detecting the participants’ dominant hand movement was utilized. The setup ensured that the sensor could accurately track a wide range of the visible hand’s positions and movements.

**3.1.1 Robotic Eye: Design and Working.** Robotic eyes, as shown in Figure 3(b), were developed to simulate human-like gazes that provide visual cues for guiding behavior and facilitating non-verbal communication. To enhance their anthropomorphic appearance, googly eye stickers were affixed to each robotic eye. The eye apparatus features two robotic eyeballs, each powered by two SG90 micro-servos. Each servo weighs 9 grams, operates at approximately 5 volts, and offers a 180-degree range of motion. This allows for 90-degree movements left, right, upward, and downward from the neutral center position. Servo movements were regulated through pulse width modulation: a 1500-microsecond pulse centers the servo at 0 degrees, a 2000-microsecond pulse achieves +90 degrees rotation, and a 1000-microsecond pulse results in -90 degrees rotation. The lower servos facilitate the yaw rotation, and the upper servos control the pitch rotation. Both eyeballs can be independently or synchronously maneuvered to gaze in any desired direction.

As depicted in the electrical schematic of the robotic eye in Figure 3(a), a Raspberry Pi 3B+ processor serves as the control unit for the yaw and pitch servo motors. General Purpose Input/Output (GPIO) pins on the Raspberry Pi directly connect to each of the four servos, enabling precise control. Each GPIO pin emits a 3.3-volt control signal that modulates the servos via pulse width modulation. Power is supplied to the servos through jumper wires from the Raspberry Pi’s positive and negative terminals to the servos’ power and ground pins on a breadboard. To maintain a visually realistic appearance, the servos were attached to 3D-printed hinge components, strategically positioned to minimize visual interference with the robotic eyeballs. In addition, a 3D printed nose and mouth structure was also



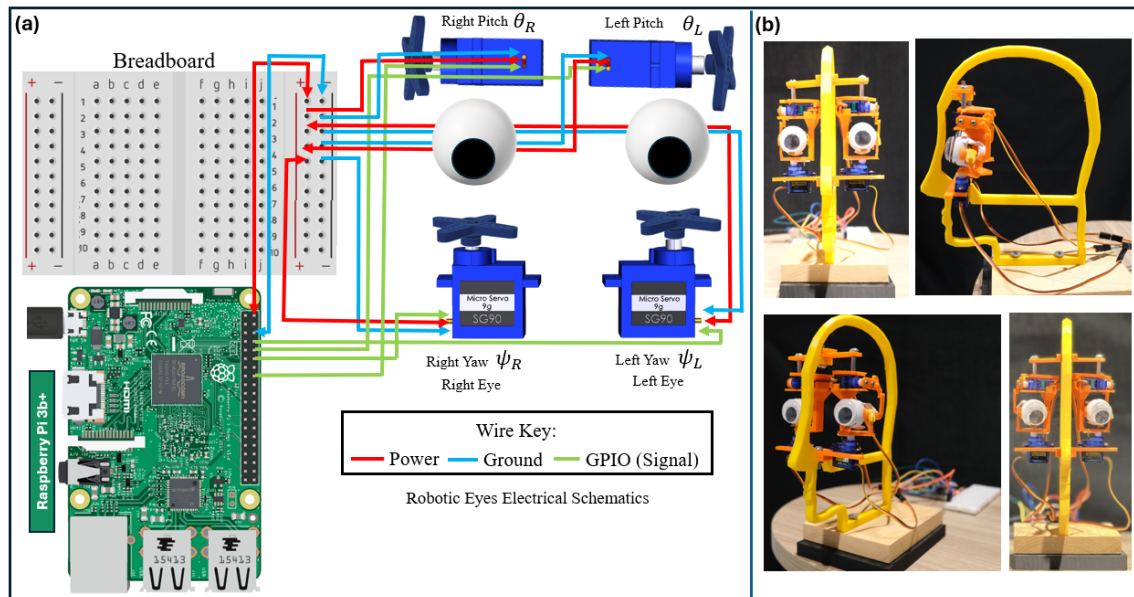


Fig. 3. (a) Electrical schematic of the robotic eyes, and (b) views of the entire robotic head from multiple angles.

integrated between motorized eyes to enhance the humanoid features of the assembly. More details on robotic eye design can be found in [25].

**3.1.2 Vision-Based Human Opinion-Tracking.** For proactive robotic actions, we observed dynamic movements of the human hand throughout each buzzer selection test using an overhead camera sensor. This sensor captures the motion frame-by-frame, with the number of frames varying along with the corresponding speed of each participant’s hand movements. To ensure robust landmark detection, we used the state-of-the-art deep learning-based hand-tracking module, MediaPipe [56], which continuously detects the 2D pose coordinates of all fingertips, knuckles, and thumbs, along with the lines connecting them. The twenty-one detected coordinates from the fingers and knuckles are averaged to derive a single midpoint pose, representing the dynamic movement of the hand pose throughout the participant interaction with the robot and decision-making process.

Additionally, the vision tracking algorithm establishes two bounding boxes around the options—blue and red buzzer buttons. Following the auditory cue “Go” from the speaker that initiates each trial of decision-making between human and robot, the algorithm analyzes the detected hand’s pose relative to the x-axis and its proximity to each bounding box, assessing the participant’s intended direction of hand movement. This real-time hand movement data is subsequently leveraged to infer dynamic human opinions as discussed in Section 4. Leveraging the captured frames and calculated human opinions, the robotic arm’s response was computed in real-time using nonlinear opinion dynamics, enabling precise control of its actions. Once the human hand pressed one of the buzzers and any of the twenty-one detected hand poses entered the bounding box of a target buzzer button, as captured by the camera sensor, the detection process and overall robot movement ceased, with the robot committing to the nearest buzzer button corresponding to the human’s choice.

### 3.2 EXPERIMENTAL PROCEDURE

At the beginning of the experiment, participants were required to sign a consent form authorizing their participation in the experiment and the use of video recordings for subsequent data analysis. The experimental procedure is described as follows:

**Step 1:** Participants were instructed to remove any hand accessories and roll up their sleeves to ensure safety and unobstructed hand pose detection by the camera. Initially, they were directed to stand on two designated black X's marked on the floor, as illustrated in Figure 4. Once the interaction began, participants were permitted to move to two designated white X's, enabling them to comfortably access the buzzer buttons.

**Remark 1:** Participants were not informed that their hand movements were being tracked, as the camera sensor was strategically positioned at a high elevation to remain unobtrusive.

**Step 2:** Following Step 1, participants were directed to hold a mechanical counter in their non-dominant hand, positioned discreetly behind their backs. Concurrently, they were required to orient their dominant hand centrally at the level of the solar plexus, extending fingers directly forward towards the robotic arm situated directly in front of them.

**Step 3:** Upon hearing the auditory countdown "1, 2, 3, GO" from a speaker, each participant was instructed to immediately move their front-positioned hand toward the red or blue buzzer button. Their objective was to press the same buzzer color as the robot at the end of each trial.

**Remark 2:** Simultaneously, to increase cognitive load, participants were tasked with pressing the mechanical counter behind their backs exactly 10 times in succession while continuing their movement toward the buzzer.

**Step 4:** During a trial, if participants press the same buzzer as the robot, they earn one point for the correct choice and an additional point for pressing the counter behind their back exactly 10 times. Failure to complete any of these tasks results in the loss of one point. Furthermore, violations of game rules specified in Remark 3 within a round will incur a one-point penalty.

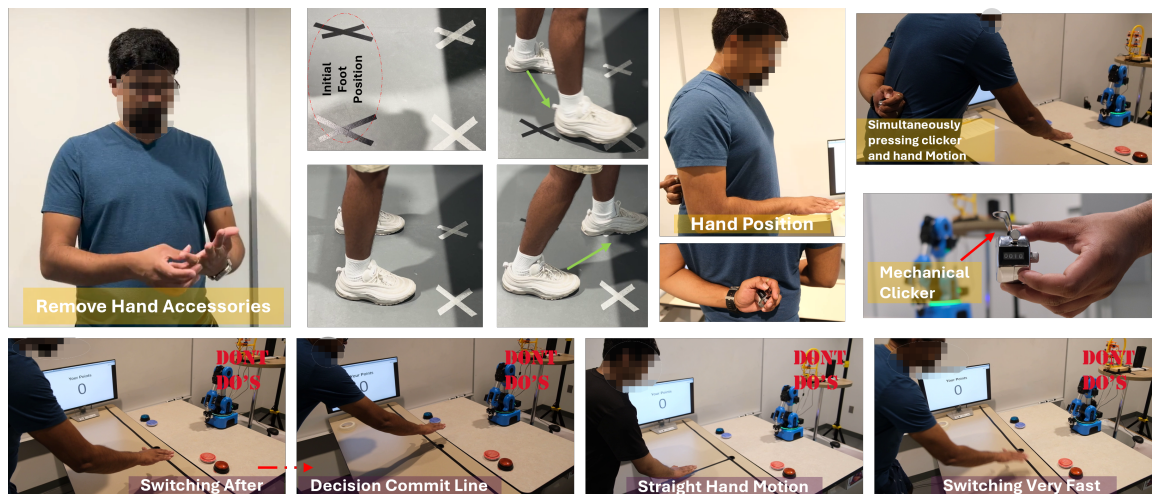


Fig. 4. Pre-experiment instructions for participants, including steps for removing hand accessories, the initial standing position with allowed stepping marks, hand positioning, and the use of a mechanical clicker for cognitive load. Illustrations of 'Don't dos' such as switching after crossing the decision line, non-straight hand use motion, and switching too quickly. (Human consent obtained for image use and identity disclosure)

**Step 5:** To match the robot’s choice in real time, participants are allowed to switch their hand path once during each trial by observing the robot’s behavior. Participants are completely unaware of the robot’s future actions, and all human and robot opinions are formed in real time during the interaction.

**Step 6:** For each participant, this decision-making interaction game was repeated for eight iterations, with potential scores ranging from a minimum of -8 to a maximum of 16 points.

**Remark 3:** Participants were not allowed to change hand paths after crossing the decision commit line. Additionally, they could switch paths only once per round and were required to maintain a constant speed during the switch.

**Step 7:** In the first three of eight trials, the robot’s behavior was strategically configured to consistently disagree from participant’s choice, ensuring it selected a different buzzer color. For instance, if the participant intended to choose red, the robot would continuously move towards blue, and vice versa. During these initial three trials, the robot’s opinion was dynamically updated in a non-linear fashion, responding to participants hand movements to consistently choose the opposite option. This configuration enabled the robot to potentially deceive the human at any moment during the interaction by adjusting its path to choose a different option, even if the human changed their path to align with the robot’s choice.

**Remark 4:** Initially, the robot’s behavior was designed to exhibit disagreement to encourage human participants to increase their effort to collaborate and increase attentiveness in the game. This approach was implemented to investigate Research Question 3.

**Step 8:** During the **first three trials, both the robot and the human were initialized with zero bias** toward any option, forming their decisions in real-time, while the robotic eye remained in a neutral position. **Beginning with the fourth trial, the robotic eye was activated to introduce a visual bias toward a specific option, thereby guiding the participant towards pressing the same buzzer color, thus developing consensus. The robot, in response, dynamically updated its internal bias, overriding the social influence of the human participant’s opinion, and systematically aligned its decision-making with the option indicated by the robotic eye.**

**Remark 5:** From the outset of the experiment, participants were not provided any information about the robotic eye—its purpose, function, or even its significance. This strategy was designed to investigate Research Question 5. Following the initial three disagreement trials, the robotic eye was autonomously activated before the fourth trial, providing continuous visual gaze cues toward one of the options until the completion of that trial. Furthermore, from the fourth to the eighth trial, the intensity of the eye’s gaze bias was progressively increased across different options to examine whether participants detected this gradual enhancement in visual cues, with the most pronounced and direct cue presented in the final, eighth trial.

At the beginning, the experimental coordinator verbally explained the entire procedure to each participant, supplemented by an instructional video illustrated in Figure 4, outlining the Do’s and Don’ts. Participants were instructed to maximize their score by selecting the same buzzer color as the robot, pressing the clicker exactly ten times, and adhering to the rules outlined in **Remark 3**.

A total of 51 participants were recruited under IRB (Project Number: 2125317) through targeted outreach and direct engagement on the university campus, with minors and individuals with a criminal history excluded. The selection process prioritized diversity in educational background, age, and gender. To ensure the authenticity and reliability of the experimental results, individuals with prior knowledge of the experimental setup, components, or robot control algorithms—which could potentially bias results—were excluded. The participants ranged in age from 18 to 55, offering a wide spectrum of perspectives and experiences. The participant pool included individuals with varied educational and professional backgrounds, from high school interns to post-doctorates, as well as working professionals across

different fields, such as campus facilities and maintenance workers, Air Force veterans, and professional athletes. There were no anticipated risks for participants, nor was there any financial compensation or prize for participation.

#### 4 BIAS-CONTROLLED NONLINEAR OPINION DYNAMICS for ROBOT BEHAVIOR REGULATION

To design the robotic eyes' behavior to communicate with human, we first need to study the interaction between the human and the robot. We model the human participant and the robot as two interacting agents. Each agent has the option of pressing a red or blue buzzer, forming their continuous opinion  $z_i \in \mathbb{R}$  with  $i \in \{r, h\}$ , where  $i = r$  represents the robot and  $h$  represents the human participant.

At any given moment during the interaction, if the opinion variable  $z_i$  satisfies that  $z_i > 0$ , agent  $i$  is predisposed to press the red buzzer; if  $z_i < 0$ , the blue buzzer is the intended choice. The magnitude  $|z_i|$  quantifies the strength of the agent's conviction towards pressing either the red or blue buzzer. Utilizing the model from [5] (equation 14), which provides a comprehensive foundation for the formation of opinions on social networks using non-linear ordinary differential equations, we define the opinion changing rate of the robot and human as  $\dot{z}_r$  and  $\dot{z}_h$ , respectively, for a two-agent, two-option opinion system. Applying a saturation function  $\hat{S}_1(y) = \tanh(y)$  in equation (14) from [5], the dynamics of the opinions are presented as follows

$$\dot{z}_r = -d_r z_r + u_r \tanh(\alpha_r z_r + \gamma_r a_{rh} z_h) + b_r, \quad (1)$$

$$\dot{z}_h = -d_h z_h + u_h \tanh(\alpha_h z_h + \gamma_h a_{hr} z_r) + b_h, \quad (2)$$

where  $d_r > 0$  and  $d_h > 0$  are decay constants representing the attenuation of opinions over time,  $u_r$  and  $u_h$  denote quantitative social influence parameters, and  $\alpha_r$  and  $\alpha_h$  are weights for self-opinion reinforcement. Parameters  $\gamma_r$  and  $\gamma_h$  represent inter-agent gains of influence on the same opinion, while  $b_r$  and  $b_h$  act as bias or external stimulus inputs for the robot and human participant, respectively. Let a matrix  $A$  denote the unweighted adjacency matrix, defined as  $A = [0, a_{rh}; a_{hr}, 0]$ , where the off-diagonal elements  $a_{rh}$  and  $a_{hr}$  represent binary directed communication edges from the robot to the human and from the human to the robot, respectively. These elements in  $A$  are set to 1 if both the robot and human continuously observe each other, and 0 otherwise [See Section II.A of [10]]. For our experiments, since the robot and the human have continuous closed-loop interaction, we can set  $a_{rh} = a_{hr} = 1$ . As a result, the eigenvalues of such an unweighted adjacency matrix  $A$  are  $\lambda_{\max} = 1$  and  $\lambda_{\min} = -1$ .

In this paper, we assume that the key parameters governing the opinion dynamics of both the human and robot are identical. This allows both agents to be treated equally as they evolve within the same decision space (red or blue buzzer). Given the bidirectional influence between the robot and the human, we assume that the system exhibits symmetry, making it behaviorally homogeneous. Thus, we model the interaction as a two-agent, two-option homogeneous system for clarity. For the rest of this subsection, we will first show how to analyze the equilibrium of the non-linear opinion dynamics with  $b_r = b_h = 0$ . The case of  $b_r \neq 0, b_h \neq 0$  is discussed in more detail in Section 4.1.

**Remark 6:** Determining the true parameters of human decision-making dynamics is beyond the scope of this paper and will be explored in future work. Additionally, while we can observe human opinions during interaction, we assume the non-linear opinion dynamics in (2) reflect internal processes in the human brain, limiting our ability to fully control human opinion formation. This is discussed in detail and illustrated in Figure 7(b) within Subsection 4.1.

By considering a homogeneous opinion system and setting  $d_r = d_h = d$ ,  $u_r = u_h = u$ ,  $\alpha_r = \alpha_h = \alpha$ ,  $\gamma_r = \gamma_h = \gamma$ . If  $b_r = b_h = 0$ , which is what has been studied in [35], a Jacobian matrix  $J$  for (1) and (2) can be derived as

$$J = \begin{bmatrix} -d + u\alpha (\operatorname{sech}(\alpha z_1 + \gamma a_{12} z_2))^2 & u\gamma (\operatorname{sech}(\alpha z_1 + \gamma a_{12} z_2))^2 \\ u\gamma (\operatorname{sech}(\alpha z_2 + \gamma a_{21} z_1))^2 & -d + u\alpha (\operatorname{sech}(\alpha z_2 + \gamma a_{21} z_1))^2 \end{bmatrix}. \quad (3)$$

Evaluating the Jacobian  $J$  from (3) at the equilibrium  $[z_r, z_h]^\top = [0, 0]^\top$  results in  $J = (-d + u\alpha)I + u\gamma A$ . Substituting  $J$  into its eigenvalue equation  $Jv = \lambda_J v$  and rearranging, we obtain the eigenvalue of  $A$  as  $\lambda = \frac{\lambda_J + d - u\alpha}{u}$ . The key results derived from [5, 35] can be summarized as below:

1. A pitchfork bifurcation occurs at critical attention point  $u = u^* = \frac{d}{\alpha + \gamma\lambda}$  where  $\lambda_J = 0$  and for  $u > u^*$  and  $\lambda_J > 0$ , the system transitions from a neutral unopinionated stable state to an opinionated unstable state, along with two stable equilibria. For  $u < u^*$  (where  $\lambda_J < 0$ ), opinions remain undecided. Conversely, for  $u > u^*$  (where  $\lambda_J > 0$ ), opinions converge towards either agreement or disagreement. This condition holds true for all initial conditions of  $z_i$ , except when  $z_r(0) = z_h(0)$ , where agents still remain in equilibrium indecision.
2. Setting  $u > u_a^* = \frac{d}{\alpha + \gamma\lambda_{\max}}$ ,  $\lambda_{\max} = \max(\lambda)$  and  $\gamma > 0$ , guarantees a consensus of opinions between the two agents.
3. And, setting  $u > u_d^* = \frac{d}{\alpha + \gamma\lambda_{\min}}$ ,  $\lambda_{\min} = \min(\lambda)$  and  $\gamma < 0$ , the opinion network is guaranteed to sustain a state of dissensus between the agents.

Before elaborating on the numerical analysis based on the preceding conclusions that ensures guaranteed disagreement and its application in our experiment, we would like to refocus the reader's attention on the overarching objective and contribution of this paper. In this work, by relaxing the small bias assumption [5, 35], we have explored dynamic bias adjustment within non-linear opinion dynamics for practical implementation in human-robot interaction, using the selected parameter set, as discussed in detail in Subsection 4.1.

We define **consensus** as  $\operatorname{sign}(z_r) = \operatorname{sign}(z_h)$  and **dissensus** as  $\operatorname{sign}(z_r) \neq \operatorname{sign}(z_h)$ . Depending on the human and robot opinions, either state can be observed at any point during the interaction. The terms "consensus" and "dissensus" are used interchangeably with "agreement" and "disagreement," respectively. This terminology reflects the focus of this research on real-world human-robot scenarios, where decision-making often involves binary choices, analogous to a strict threshold for selecting or rejecting an option.

As outlined in **Step 7** of the experimental procedure in Section 3.2, the robot's behavior was deliberately configured to induce simulated disagreement during the **first three** of eight trials by consistently selecting the buzzer color opposite to the participant's choice. This can be achieved by setting  $u > u_d^*$ ,  $\lambda_{\min} = -1$ , and  $\gamma < 0$ , with both the human and robot bias parameters set to  $b_r = b_h = 0$ . The system parameters listed in TABLE I, including  $d$ ,  $u$ ,  $\alpha$ ,  $\gamma$ , and other key variables, were optimized for these three disagreement trials through an iterative hit-and-trial experimental approach. These parameters will first be used for the theoretical analysis of a two-agent, two-option opinion system in this section and later applied in the human-robot interaction experiment presented. It is important to note that for any specific human-robot interaction scenario, precise tuning of these parameters, either through analytical methods or iterative experimentation, is essential to ensure both effective operation and optimal performance.

TABLE I: EXPERIMENTAL AND THEORETICAL ANALYSIS PARAMETERS FOR NON-LINEAR OPINION DYNAMICS

Parameters	Homogeneous Opinion System Two-agent Two-option (Parameters for Theoretical Analysis) (Equations: 1, 2, 13, 14)		Robot Opinion Experimental Parameters (Equations: 1, 13)		Human Opinion Observation Experimental Parameters (Equation: 15)
	Disagreement Trials (1 to 3)	Bias Controlled Trials (4 to 8)	Disagreement Trials (1 to 3)	Bias Controlled Trials (4 to 8)	
	$(d_r = d_h = d, u_r = u_h = u, \alpha_r = \alpha_h = \alpha, \gamma_r = \gamma_h = \gamma, b_r^* = b_h^* = b^*, a_{rh} = a_{hr} = 1)$		$(d_r = d, u_r = u, \alpha_r = \alpha, \gamma_r = \gamma, a_{rh} = 1, b_r^* = b^*)$		
$d$	10.00	10.00	10.00	10.00	-
$u$	2.24	2.24	2.24	2.24	-
$\alpha$	0.05	0.05	0.05	0.05	-
$\gamma$	-8.00	-8.00	-8.00	-8.00	-
$b^*$	-	3.24	-	3.24	-
$ \sigma $	-	0.1	-	0.1	-
$k$	-	16	-	16	-
$a$	-	-	-	-	8
$x$	-	-	-	-	1.5

For the first three trials with  $b_r = b_h = 0$ , non-linear opinion system has an equilibrium ( $\dot{z}_r = \dot{z}_h = 0$ ) with homogeneous parameters. We can rearrange equations (1) and (2) into the following form given in (4) and (5):

$$\tanh(\alpha z_r + \gamma z_h) = \frac{d}{u} z_r, \quad (4)$$

$$\tanh(\alpha z_h + \gamma z_r) = \frac{d}{u} z_h. \quad (5)$$

To find the number of equilibrium solutions of the coupled non-linear system, we compute the differences between the left-hand side (LHS) and right-hand side (RHS) of equations (4) and (5). This gives us the following expressions (6) and (7):

$$\Delta_1|_{b_r=b_h=0}(z_r, z_h) = \tanh(\alpha z_r + \gamma z_h) - \frac{d}{u} z_r, \quad (6)$$

$$\Delta_2|_{b_r=b_h=0}(z_r, z_h) = \tanh(\alpha z_h + \gamma z_r) - \frac{d}{u} z_h. \quad (7)$$

By plotting the zero-level contours of  $\Delta_1|_{b_r=b_h=0}(z_r, z_h)$  and  $\Delta_2|_{b_r=b_h=0}(z_r, z_h)$  in the  $(z_r, z_h)$  plane, as shown in Figure 5(a), we identified the loci where each equation is independently satisfied. The intersection points of these contours correspond to the values of  $z_r$  and  $z_h$  that satisfy both equations simultaneously, representing the equilibrium solutions of the system. Since the equilibrium points occur at  $\Delta_1|_{b_r=b_h=0}(z_r, z_h) = 0$  and  $\Delta_2|_{b_r=b_h=0}(z_r, z_h) = 0$ , the number of intersection points indicates the number of equilibrium solutions. From Figure 5(a), specifically for the parameter set presented in TABLE I for disagreement trials (1–3), we observe three equilibrium solutions: two stable disagreement equilibria where  $\text{sgn}(z_r) \neq \text{sgn}(z_h)$ , and one unstable equilibrium where both opinions are neutral. Additionally, as discussed in [5], when the social attention parameter  $u$  exceeds the critical threshold  $u_d^* = \frac{d}{\alpha + \gamma \lambda_{\min}}$ , the system undergoes a pitchfork bifurcation, transitioning from one to three equilibrium solutions. Thus, the parameters

chosen for disagreement trials in TABLE I place the system in a state where three equilibrium solutions are already present.

For subsequent trials, beginning with the fourth, the experimental protocol was designed to facilitate a transition from disagreement to agreement. Under the sustained conditions of  $u > u_d^*$  and  $\gamma < 0$ , which promote disagreement between human and robot, the theoretical analysis in Section 4.1 will explain the mechanisms that can lead to consensus, ultimately enabling coordinated actions, such as the selection of the same buzzer color by both agents. In Section V.C of [5], the authors proposed the ‘Dynamics on weight’ approach, described by (8), which models the dynamics of  $\gamma$  to facilitate transitions between disagreement and agreement. Here,  $(\hat{x}_1, \hat{x}_2)$  represent the opinions of two agents, corresponding to  $(z_r, z_h)$  in this paper, with the function  $S_\gamma(y) = \gamma_f \tanh(g_\gamma y)$ , where  $\gamma_f > 0$  and  $g_\gamma > 0$ . The sign of the design parameter  $\sigma$  in (8) determines whether the system tends toward agreement ( $\sigma = 1$ ) or disagreement ( $\sigma = -1$ ), allowing transitions between these states. However, in the human-robot interaction and decision-making experiment presented in Section 3, quantifying or controlling the influence of a robot on human opinion formation, represented by the  $\gamma$  parameter, or vice versa, poses significant challenges and lacks intuitive application for facilitating consensus transitions.

$$\tau_\gamma \dot{\gamma}_i = -\gamma_i + \sigma S_\gamma(\hat{x}_1 \hat{x}_2) \quad (8)$$

Furthermore, employing the dynamics of  $\dot{\gamma}$  to facilitate these transitions may result in the agents remaining unopinionated under certain model parameters, due to the strong dependency of the opinionated conditions  $u > u^* = \frac{d}{\alpha + \gamma \lambda}$  on the parameter  $\gamma$ .

#### 4.1 Two-agent Two option Homogeneous Opinion system: Numerical Analysis of System Behaviour for Bias Controlled Transition to Consensus

For fully controlled and practically applicable consensus transitions from disagreement to agreement, we propose utilizing bias parameters  $b_r$  and  $b_h$ . Previous work, such as [2, 5, 6], considers cases with nonzero bias and presents results on the unfolding of the bifurcation behaviour. These results generally hold as long as the biases remain small in the topological neighborhood sense. However, the behavior of the model is well understood only for small biases. In contrast, this research departs from the small bias assumption, exploring dynamic bias adjustment for practical use within a chosen parameter set, enabling transitions from disagreement to consensus between two homogeneous agents. This approach is ultimately intended for application in the presented human-robot interaction experiment.

Now, to explore transitions from disagreement to agreement using bias as a control stimulus, we analyzed the behavior of the opinion dynamics system under varied bias conditions. This analysis involved numerical simulations, including parameter sweeping, identifying the number of equilibrium solutions across different bias values, and conducting a continuation analysis of the equilibrium, as detailed in the following subsections.

**4.1.1 Parameter Sweep Across Bias :** Systematic sweeps of the bias parameters  $b_r$  and  $b_h$  within the range  $[-6, 6]$  are conducted under the pre-configured settings  $u > u^* = \frac{d}{\alpha + \gamma \lambda_{\min}}$  and  $\gamma < 0$ , ensuring disagreement for the parameter set shown in the disagreement trial (1 to 3) in TABLE I. As shown in Figure 5(b), for the critical threshold  $u$ , the bias pair  $(b_r, b_h)$  must exceed the boundaries of a square, indicated by a white dashed line, centered at  $(0, 0)$  with a side length of  $2u$ . Furthermore, to achieve agreement after transitioning from the square region, both biases must have the same sign, i.e.,  $\text{sign}(b_1) = \text{sign}(b_2)$ , where  $\text{sign}(x) = -1$  if  $x < 0$ ,  $\text{sign}(x) = 0$  if  $x = 0$ , and  $\text{sign}(x) = 1$  if  $x > 0$ . Consensus is reached when the biases of both the human and the robot share the same sign:  $\text{sign}(b_r) = \text{sign}(b_h) = 1$ , results in both pressing the red buzzer, while  $\text{sign}(b_r) = \text{sign}(b_h) = -1$ , leads to both selecting the blue buzzer.

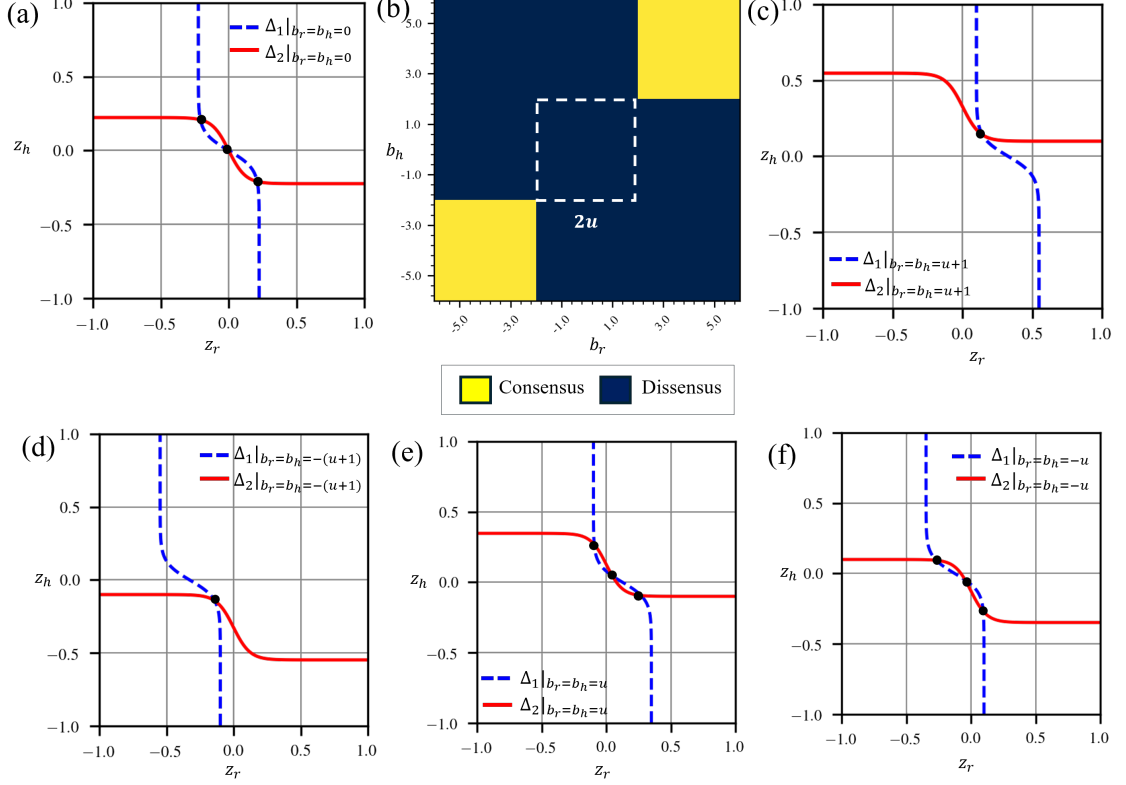


Fig. 5. Analysis showing: (a) Zero-level contours for  $\Delta_1$  and  $\Delta_2$  with biases  $b_r = b_h = 0$  and other parameters set as per TABLE 1. The intersection of the contours illustrates three equilibrium points, corresponding to equations (6) and (7), with both agents showing disagreement. (b) Single-parameter sweep of  $b_r$  with consensus and dissensus regions shown in yellow and blue, respectively.  $b_h$  is held constant at  $u + 1 = 2.24 + 1 = 3.24$ . (c) Zero-level contours for  $\Delta_1$  and  $\Delta_2$  showing only one equilibrium solution for non-zero biases, where  $b_r = b_h = u + 1 = 3.24$ . (d) Zero-level contours for  $\Delta_1$  and  $\Delta_2$ , again showing one equilibrium solution for  $b_r = b_h = -(u + 1) = -3.24$ . (e) Zero-level contours illustrating three equilibrium points for  $b_r = b_h = u = 2.24$ . (f) Zero-level contours illustrating three equilibrium points for  $b_r = b_h = -u = -2.24$ .

**4.1.2 Equilibrium Point Multiplicity: Multi-stability in Phase Space? :** Now, to determine the number of equilibrium solutions and possible bifurcation behavior under varying biases  $b_r$  and  $b_h$ , for the parameter set  $d = 10$ ,  $\alpha = 0.05$ , and  $\gamma = -8$ , in the disagreement setting  $u = u^* + 1 = \frac{d}{\alpha + \gamma\lambda} + 1 = 2.24$ , we analyze the system at equilibrium where  $b_r \neq 0$  and  $b_h \neq 0$ . Rearranging (1) and (2), we obtain (9) and (10).

$$\Delta_1|_{b_r \neq 0, b_h \neq 0}(z_r, z_h) = \tanh(\alpha z_r + \gamma z_h) - \frac{dz_r - b_r}{u}, \quad (9)$$

$$\Delta_2|_{b_r \neq 0, b_h \neq 0}(z_r, z_h) = \tanh(\alpha z_h + \gamma z_r) - \frac{dz_h - b_h}{u}. \quad (10)$$

By plotting the zero-level contours of  $\Delta_1|_{b_r \neq 0, b_h \neq 0}(z_r, z_h)$  and  $\Delta_2|_{b_r \neq 0, b_h \neq 0}(z_r, z_h)$  in the  $(z_r, z_h)$  plane, we can identify the loci where each equation is satisfied independently. The intersection points represent the equilibrium solutions of the system. Since the equilibrium points occur at  $\Delta_1|_{b_r \neq 0, b_h \neq 0}(z_r, z_h) = 0$  and  $\Delta_2|_{b_r \neq 0, b_h \neq 0}(z_r, z_h) = 0$ , the number of intersection points indicates the number of equilibrium solutions. From Figure 5(c), where  $u = 2.2422$  and



$b_r = b_h = 3.2422$ , and Figure 5(d), where  $u = 2.2422$  and  $b_r = b_h = -3.2422$ , we observe that in both cases, there is only one unique equilibrium solution. However, in Figures 5(e) and 5(f), with  $u = 2.2422$ ,  $b_r = b_h = 1.2422$  and  $u = 2.2422$ ,  $b_r = b_h = -1.2422$ , respectively, we observe three equilibrium solutions in both cases. From these observations, we conclude that for our parameter set, when the magnitudes of biases  $b_r$  and  $b_h$  are greater than the social attention parameter  $u$ , and both biases have the same sign, there is only one unique equilibrium point. To help readers better understand the concept, we consider a simplified one-agent, two-option opinion model as given in (11). This model demonstrates the same mechanism leading to a single unique equilibrium.

$$\dot{z} = -dz + u \tanh(\alpha z) + b, \quad (11)$$

At equilibrium, where  $\dot{z} = 0$ , (11) can be rearranged to (12):

$$\tanh(\alpha z) = \frac{d}{u}z - \frac{b}{u}. \quad (12)$$

The  $\tanh(\alpha z)$  function in (12), is plotted alongside a straight line with an intercept of  $-\frac{b}{u}$  and a slope of  $\frac{d}{u}$ . For the parameter values  $d = 10$ ,  $\alpha = 15$ , and  $u > \frac{d}{\alpha}$ , with  $u = 1.66$  and  $b = 2.66$  such that  $b > u$ , the number of equilibrium solutions is determined by the intersection points of the  $\tanh(\alpha z)$  curve and the linear equation  $\frac{d}{u}z - \frac{b}{u}$ . As illustrated in Figure 6(a), the curves intersect at only one point, confirming the existence of a unique equilibrium solution. For our homogeneous coupled two-agent, two-option opinion system at equilibrium, described by (9) and (10), the behavior remains consistent, showing a single equilibrium solution. However, due to the strong inter-connectivity between agents, we utilize zero-level contour plots instead of 3D tanh surface plots, as demonstrated for the simplified model in (11) with 2D tanh and line plots. Numerical analysis indicates that there is a single unique equilibrium solution for the parameter set in TABLE I (Bias-controlled trials 4 to 8). Furthermore, evaluating the eigenvalues  $-3.83$  and  $-16.08$ , of the Jacobian matrix  $[-9.96, -6.12; -6.12, -9.96]$  for equations (1) and (2) at this equilibrium point confirms the stability of the system.

**Note:** The claim of a single unique equilibrium presented above is valid for the selected parameters, which are specifically optimized for our human-robot interaction experimental setup. However, the bias parameters can exhibit multi-stable, multi-phase equilibrium solutions or display bifurcation behaviors, such as saddle-node bifurcations. A detailed analysis of such bifurcation behavior is beyond the scope of this paper. For further details, please refer to [2].

**4.1.3 Continuation Analysis of the Unique Stable Equilibrium Under Varying Bias:** To rigorously analyze the influence of bias on equilibrium behavior, a continuation analysis was conducted for the unique equilibrium (justified in Subsection 4.1.2) of opinions  $z_r$  and  $z_h$ . For the parameter set provided in TABLE I, during the disagreement trials (1-3), continuation analysis is performed under two scenarios: (1) modulating the robot bias  $b_r$  while keeping the human bias fixed at  $b_h = u + 1 = 2.24 + 1 = 3.24$ , and (2) varying both  $b_h$  and  $b_r$  concurrently. As shown in Figure 6(b), when  $b_r$  is varied within the range  $[-5, 10]$ , the initial configuration  $b_r < u$  results in disagreement in the equilibrium opinions  $z_r^*$  and  $z_h^*$ , where  $\text{sgn}(z_r^*) = -1 \neq \text{sgn}(z_h^*)$ . However, at the critical point  $b_r = u$ ,  $z_r^*$  crosses the x-axis and becomes positive. Beyond this threshold, for  $b_r > u$ , both opinions align, resulting in agreement with  $\text{sgn}(z_r^*) = \text{sgn}(z_h^*) = 1$ , leading to consensus.

We also simulate the dual parameter variation for human bias  $b_h$  and robot bias  $b_r$  within the range  $[-10, 10]$ . In Figure 6(c), where  $b_r$  and  $b_h$  vary equally, it is evident from the equilibrium behavior of  $z_r^*$  and  $z_h^*$  that when  $b_r$  and  $b_h$  exceed the social attention parameter  $u$ , both opinion equilibria reach consensus and transition to a positive state (indicating the red buzzer). Conversely, when  $b_r$  and  $b_h$  are less than  $-u$ , the opinion equilibria transition to a negative

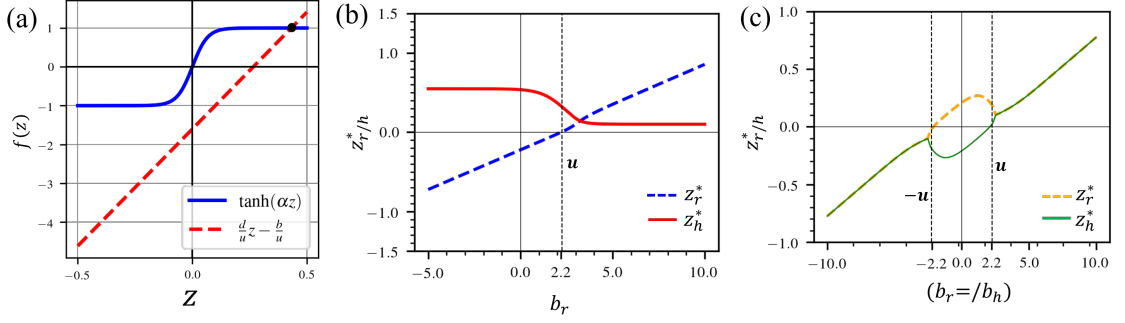


Fig. 6. (a) Plot of the  $\tanh(\alpha z)$  curve along with the straight line  $\frac{d}{u}z - \frac{b}{u}$ . The intersection point represents the number of equilibrium solutions, which is one in this case (corresponding to equation 12). (b) Continuation analysis of the single equilibrium points  $z_r^*$  and  $z_h^*$ , with the parameter  $b_r$  varying while other parameters are fixed as per Table 1 (disagreement trials 1 to 3). The illustration shows that as  $b_r > u$ ,  $z_r^*$  and  $z_h^*$  reach consensus. (c) Continuation analysis of the opinion equilibria  $z_r^*$  and  $z_h^*$  when both  $b_r$  and  $b_h$  are varied equally.

state (indicating the blue buzzer). Additionally, based on the analysis in Figures 6(b) and 6(c), the computed eigenvalues of the Jacobian matrix are negative, indicating that the system is stable at this unique equilibrium.

Summarizing our insights from the numerical analysis and the opinion behavior under dynamic bias conditions, we conclude that for  $b_r > u_r$  and  $b_h > u_h$  (where  $u_r = u_h$  allows for a single value  $u$ , otherwise distinct symbols  $u_r$  and  $u_h$  are used), there exists a single equilibrium point, leading to agreement toward the red buzzer. Conversely, for  $0 < b_r < u_r$  and  $0 < b_h < u_h$ , the result is disagreement. Similarly, for  $b_r < -u_r$  and  $b_h < -u_h$ , there is one equilibrium point leading to agreement towards the blue buzzer, while for  $-u_r < b_r < 0$  and  $-u_h < b_h < 0$ , the result is again disagreement. Based on these insights from the parameter sweep, equilibrium point multiplicity determination, and continuation analysis, we can state that within our experimental framework—where a human participant and a robot act as two agents choosing between a red and blue buzzer, each modeled by opinion dynamics with the parameter set provided in TABLE I for the disagreement trials (1 to 3)—a transition from disagreement to agreement in their opinions ( $z_r, z_h$ ) can only occur if the following conditions on both human and robot biases are met:

- (1) The biases of the human and robot agents,  $b_r$  and  $b_h$ , must have the same sign, i.e.,  $\text{sign}(b_r) = \text{sign}(b_h)$ .
- (2) The magnitudes of these biases,  $|b_r|$  and  $|b_h|$ , must exceed their respective critical bias (attention) thresholds  $b_r^*$  and  $b_h^*$ , defined as  $b_i^* = u_i^* > \frac{d_i}{\alpha_i + \gamma_i \lambda_{\min}} > 0$  for  $i \in \{r, h\}$ , i.e.,  $|b_r| > b_r^*$  and  $|b_h| > b_h^*$ . Specifically:
  - For agreement on the red buzzer ( $\text{sign}(z_r), \text{sign}(z_h) \in \{+\}$ ), both biases  $b_r$  and  $b_h$  must be positive,  $\text{sign}(b_r) = \text{sign}(b_h) = +1$ .
  - For agreement on the blue buzzer ( $\text{sign}(z_r), \text{sign}(z_h) \in \{-\}$ ), both biases  $b_r$  and  $b_h$  must be negative,  $\text{sign}(b_r) = \text{sign}(b_h) = -1$ .

To achieve this transition to consensus from dissensus under stated bias conditions, we present dynamic biases models  $\dot{b}_r$  and  $\dot{b}_h$ , presented in (13) and (14).

$$\dot{b}_r = \sigma \cdot z_r \cdot \text{sgn}(z_h) + \alpha \cdot \max(0, b_r^* - |b_r|), \quad (13)$$

$$\dot{b}_h = \sigma \cdot z_h \cdot \text{sgn}(z_r) + \alpha \cdot \max(0, b_h^* - |b_h|), \quad (14)$$

The first terms  $\sigma \cdot z_r \cdot \text{sgn}(z_h)$  and  $\sigma \cdot z_h \cdot \text{sgn}(z_r)$  in biases dynamics align the signs of  $b_r$  and  $b_h$  according to the selected agreement option to press red or blue. This term effectively merges two perspectives or viewpoints, reducing potential conflicts by leveraging the interaction of the opinions  $z_r, z_h$ . The second terms,  $\alpha \cdot \max(0, b_r^* - |b_r|)$  and  $\alpha \cdot \max(0, b_h^* - |b_h|)$ , work to elevate the biases  $b_r$  and  $b_h$  above their designated thresholds  $b_r^*$  and  $b_h^*$  respectively. These thresholds are defined such that  $b_r^* = u_r^* > \frac{d_r}{\alpha_r + \gamma_r \lambda_{\min}} > 0$  and  $b_h^* = u_h^* > \frac{d_h}{\alpha_h + \gamma_h \lambda_{\min}} > 0$ , ensuring that the biases exceed values required for maintaining the stability of agreement dynamics. The proposed bias dynamics model draws on real-world intuition and shows that the inclination to favor a specific option—red or blue—intensifies when the biases  $b_r$  and  $b_h$ , corresponding to robot and human agents, respectively, surpass the maximum impact of collective social influence exerted by their counterparts. This influence is quantitatively expressed as  $u_r \tanh(\alpha_r z_r + \gamma_r z_h)$  and  $u_h \tanh(\alpha_h z_h + \gamma_h z_r)$ , where the maximum value of both  $\tanh(\alpha_r z_r + \gamma_r z_h)$  and  $\tanh(\alpha_h z_h + \gamma_h z_r)$  is 1. Consequently, when both  $b_r$  and  $b_h$  exceed their respective attention thresholds  $u_r$  and  $u_h$ , the opinion dynamics progressively align with the selected biased option, reflecting a deeper integration of individual and collective preferences.

**Remark 7:** We need the dynamic model for  $b_r$  and  $b_h$ , rather than simply configuring the initial settings by assigning static  $b_r = |u_r| + b_r$  and  $b_h = |u_h| + b_h$ , as such settings would place the opinion system in agreement from the outset of the formation of the opinions. Also, these static bias configurations contradict the primary goal of this research, which is to allow dynamic bias to evolve over time when a disagreement between agents is detected, leading the opinions to reach a consensus naturally. Furthermore, human biases are not static in the real world but form, evolve, and dissipate over time based on accumulating evidence [43, 65]. This underscores the need for a dynamic bias model presented in (13) and (14), which can be used as dynamic control to drive the system toward consensus. Additionally, the use of the sign function  $\text{sgn}(\cdot)$  in the dynamic models for  $b_r$  and  $b_h$  introduces discontinuities. In our experimental setup, this discontinuity is acceptable, as it reflects the abrupt switching behavior commonly observed in human-robot interactions. The sign function captures critical switching behaviors and decision boundaries essential for modeling such interactions. Smoothing the discontinuity would not accurately represent the phenomena of interest. In future work, a detailed analysis of the discontinuity and continuity in the dynamic bias models will be conducted using Filippov solutions [16].

Although it is anticipated that human internal decision-making adheres to non-linear opinion dynamics given in (2), which effectively incorporate elements such as memory retention of previous choices, non-linear social attention to robotic inputs, and the influence of external biases, however, direct control over human opinion is not feasible. Only observation of human opinion is possible during interactive settings, as Figure 7(b) illustrates. Consequently, to facilitate the empirical observation of human opinions during these interactions, we propose a model outlined in (15):

$$z_h = a \cdot \cos(\theta) \cdot \tanh\left(\frac{k}{d}\right) \quad (15)$$

where  $z_h$  quantifies the observed human opinion. The term  $a \cdot \cos(\theta)$  calculates the directional intent of the human opinion towards a specific option, where  $\theta$  is the angle between the human movement vector and the x-axis as shown in Figure 7(a). Additionally, the hyperbolic tangent function,  $\tanh\left(\frac{k}{d}\right)$ , modulates the intensity of the opinion based on the normalized distance  $d$  from the human hand to the target buzzers. The parameters  $k$  and  $a$  are scaling weights that adjust the influence of distance and directional intent, respectively.

Algorithm 1 provides a detailed description for observing human opinion and forming robotic opinion during interactions. It takes inputs from a real-time overhead camera feed capturing human hand gestures and detects a complete set of hand landmarks  $\{(x_i, y_i)\}_{i=1}^N$  utilizing MediaPipe [56]. These landmarks, along with the formed robotic opinion  $z_r$ , are transmitted to Algorithm 2, which then controls robot actions. Furthermore, Algorithm 1 calculates the

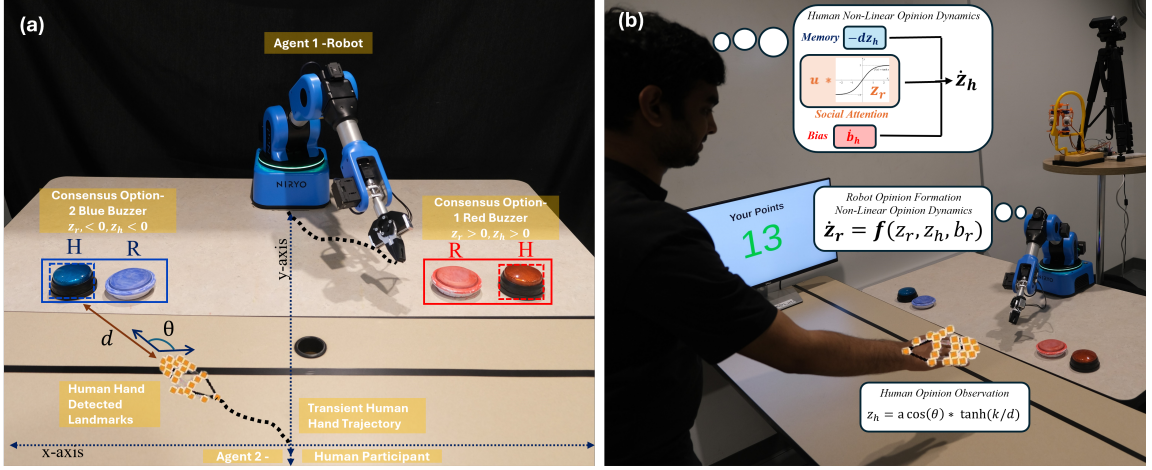


Fig. 7. (a) Illustration of the calculation of the angle  $\theta$  and distance  $d$  for human opinion observation, showing how the robot captures and interprets the human's decision-making process. (b) Illustration of a comprehensive mental model integrating human internal opinion dynamics, observed opinion dynamics, and the robot's non-linear opinion dynamics, demonstrating how the decision-making process is anticipated during interaction.

norm of the human hand movement vector  $\|\mathbf{M}\|$  using the current position vector  $\mathbf{p}(t)$  and the immediately preceding position vector  $\mathbf{p}_{-1}(t)$ .

Utilizing the movement vector  $\mathbf{M}$ ,  $\theta$  is computed and normalized to restrict its range to the first and second quadrants, aligning the calculation of opinions with the choice of either the red or blue buzzer. If  $\theta$  lies within  $[\frac{\pi}{2}, \pi)$ ,  $d$  quantifies the distance to the blue buzzer, indicating a directional intent towards it. Conversely, when  $\theta$  is within  $[0, \frac{\pi}{2})$ ,  $d$  measures proximity to the red buzzer, thus determining the targeted buzzer based on hand orientation. Across trials 1 to 8, the observed human opinion  $z_h$  and robot opinion  $z_r$  are determined, with the robot's non-linear opinion dynamics configured to  $u_r > u_d^* = \frac{d}{\alpha + \gamma \lambda_{\min}}$ , where  $\gamma < 0$  intentionally promotes disagreement with human opinions. However, from the 4<sup>th</sup> to the 8<sup>th</sup> trial, the **Bias Consensus Algorithm** is activated, dynamically adjusting the robot's opinion  $z_r$  and bias  $b_r$  based on (13) toward the initially inputted consensus option  $O$  in Algorithm 1. The utilized parameters for the dynamic bias model  $b_r$ , along with the opinion dynamics  $\dot{z}_r$  and  $z_h$ , are provided in TABLE I.

**Remark 8:** The Bias Consensus algorithm will terminate when the human and robot opinions reach consensus, i.e., when  $z_r \cdot z_h > 0$ . Until this condition is met, the algorithm continuously increases the robot bias  $b_r$  beyond the critical threshold  $b_r^*$ , ensuring that the signs of  $z_r$  and  $z_h$  become identical at each point during the interaction. Once consensus is achieved, the dynamics ensure that the robot bias  $b_r$  remains in the desired state by continuously monitoring the bias and adjusting the robot's opinion accordingly. Concurrently, visual cues from the robotic eye are activated to impart bias in human opinion toward the same consensus option  $O$ . A detailed mechanism of the gradual increase in visual cues from robotic eyes is discussed in Section 5.

Algorithm 2 receives  $z_r$  and the set of detected hand landmarks  $\{(x_i, y_i)\}_{i=1}^N$  from Algorithm 1. It then initializes the opinion change vector  $\vec{T}$  and the change count  $C$ . To ensure robustness and safety, the robot only alters its actions if every element within  $\vec{T}$  transitions to true and  $C$  exceeds the maximum change threshold  $C_{\max}$ . Based on the initial value of  $\text{sgn}(z_r)$ , the robot decides its movement action, either towards the red or blue buzzer.

---

**Algorithm 1:** Human Opinion Observation and Robot Opinion Formation Algorithm

---

**Input:**  $O \in \{\text{"red"}, \text{"blue"}\}$ , Real-time overhead camera feed of human hand gestures

*// Input  $O$  for trials 4 to 8, denoting the common consensus option.*

**Output:** **Robot Action** in Algorithm 2

**Data:**  $\mathbf{p}_{\text{buzzer}} = \{\text{"blue"} : [(x_{1b}, y_{1b}), (x_{2b}, y_{2b})], \text{"red"} : [(x_{1r}, y_{1r}), (x_{2r}, y_{2r})]\}$

*// Position vector of red and blue buzzers bounding boxes relative to hand pose*

**Trigger:** Audio signal "1, 2, 3, ... go"

```

1 while true do
2   I = cv2.VideoCapture().read() // Reading human hand video feed using OpenCV
3    $\{(x_i, y_i)\}_{i=1}^N \leftarrow \text{mediapipe\_detection}(I)$  // Detects  $N$  2D landmarks on entire hand
4    $\mathbf{p}(t) = \left[ \frac{1}{N} \sum_{i=1}^N x_i, \frac{1}{N} \sum_{i=1}^N y_i \right]^T$  // Compute current hand position vector
5    $\mathbf{p}(t-1) = \left[ \frac{1}{N} \sum_{i=1}^N x_{i,t-1}, \frac{1}{N} \sum_{i=1}^N y_{i,t-1} \right]^T$  // Previous hand position vector
6    $\mathbf{M} = \mathbf{p}(t) - \mathbf{p}(t-1)$  // Human hand movement vector
7    $\|\mathbf{M}\| = \sqrt{\mathbf{M}^T \mathbf{M}}$  // Compute norm of movement vector
8    $\theta = \arctan 2(-\mathbf{M}_y, \mathbf{M}_x)$  // Calculate angle with x-axis
9    $\theta = \theta - 2\pi \cdot \left\lfloor \frac{\theta}{2\pi} \right\rfloor$  // Adjust  $\theta$  to be non-negative and less than  $2\pi$ 
10  if  $\frac{3\pi}{2} \leq \theta < 2\pi$  then
11    |  $\theta = \pi - (2\pi - \theta)$  // Mirror  $\theta$  to second quadrant
12  else if  $\pi \leq \theta < \frac{3\pi}{2}$  then
13    |  $\theta = \theta - \pi$  // Shift  $\theta$  to first quadrant
14  if  $\frac{\pi}{2} \leq \theta < \pi$  then
15    |  $d = \|\mathbf{p}(t) - \mathbf{p}_{\text{buzzer}}[\text{"blue"}][0]\|$  // Distance of hand pose to blue buzzer
16  else if  $0 \leq \theta < \frac{\pi}{2}$  then
17    |  $d = \|\mathbf{p}(t) - \mathbf{p}_{\text{buzzer}}[\text{"red"}][0]\|$  // Distance of hand pose to red buzzer
18   $z_h = a \cdot \cos(\theta) \cdot \tanh(k/d)$  // Observe human opinion  $z_h$  based on  $d$  and  $\theta$ 
19   $\dot{z}_r = -d_r z_r + u_r \tanh(\alpha_r z_r + \gamma_r z_h) + b_r$  // Formulates robot opinion  $z_r$  under persistent disagreement conditions
    where  $u_r > u_d^* = \frac{d}{\alpha + \gamma \lambda_{\min}}$ , and,  $\gamma < 0$ .
20  Bias Consensus Algorithm (Activated for only trial 4 to 8)
21  while  $z_r \cdot z_h < 0$  do
22    | if  $O = \text{"Red"}$  then  $\sigma \leftarrow -1$ 
23    | else  $\sigma \leftarrow +1$ 
24    |  $\alpha = -K \cdot \sigma$  // Define  $\alpha$  in terms of  $K$  and  $\sigma$ 
25    |  $\dot{b}_r = \sigma(z_r \cdot \text{sgn}(z_h) - K \cdot \max(0, b_r^* - |b_r|))$  // Adjust  $b_r$  dynamics
26    |  $\dot{z}_r = -d_r z_r + u_r \tanh(\alpha_r z_r + \gamma_r z_h) + b_r$  // Update  $z_r$  dynamics
27  On Exit (When  $z_r \cdot z_h > 0$ ) // Consensus achieved
28  |  $\dot{b}_r \leftarrow 0$  // Stop updating  $b_r$ 
29 Transmit:  $z_r, \{(x_i, y_i)\}_{i=1}^N$ , and  $\mathbf{p}_{\text{buzzer}}$  to Algorithm 2.

```

---

If  $\text{sgn}(z_r)$  transitions from +1 to -1 or vice versa, the robot requires  $C_{\max}$  consecutive identical  $\text{sgn}(z_r)$  values, either +1 or -1, to confirm a stable directional change before adjusting its trajectory. This mechanism ensures that the robot does not respond to abrupt, transient shifts in human opinion, thereby stabilizing interaction. Once  $C \geq C_{\max}$ , both  $\vec{T}$  and  $C$  are reset to their initial states for the subsequent change evaluation. The robot then pauses for 0.1 seconds and adjusts its course towards the red or blue option based on the trial number. In trials 1 to 3, designed for disagreement, the robot selects the opposite option; in trials 4 to 8, dynamic bias adjustments override initial disagreements, directing

**Algorithm 2:** Non-Linear opinion dynamics based Robot behaviour control algorithm

---

```

1 Receive:  $z_r$ ,  $\{(x_i, y_i)\}_{i=1}^N$ , and  $\mathbf{p}_{\text{buzzer}}$  from Algorithm 1.
2 Initialize:  $\vec{T} \leftarrow [False, False, False]$ ,  $C \leftarrow 0$ ,  $C_{\max} \leftarrow 4$ 
   // Initialize opinion change vector  $\vec{T}$ , change count  $C$  and max change count  $C_{\max}$  required in robot opinion  $z_r$  to
   // switch its path towards alternative option.
3  $\sigma_{\text{sgn}(z_r)} \leftarrow 0$ ,  $\sigma_{\text{sgn}(z_r)} \in \{-1, +1, 0\}$  //  $\sigma_{\text{sgn}(z_r)}$  is preceding value of  $\text{sgn}(z_r)$ 
4 while true do
5   if  $\sigma_{\text{sgn}(z_r)} = 0$  then
6     if  $\text{sgn}(z_r) = +1$  then
7       | Robot Action: Move Towards Red // Move through first value of  $\text{sgn}(z_r)$ 
8     else
9       | Robot Action: Move Towards Blue // Move through first value of  $\text{sgn}(z_r)$ 
10     $\sigma_{\text{sgn}(z_r)} \leftarrow \text{sgn}(z_r)$  // Update sign for the next cycle
11  if  $\sigma_{\text{sgn}(z_r)} \neq 0$  and  $\sigma_{\text{sgn}(z_r)} \neq \text{sgn}(z_r)$  then
12    |  $C \leftarrow C + 1$  // Increment change counter on  $z_r$  sign change
13    |  $\vec{T}[0] \leftarrow \text{True}$  // Mark the first transition state
14  if  $\sigma_{\text{sgn}(z_2)} \neq 0$  then
15    for  $i \leftarrow 0$  to 1 do
16      | if  $\vec{T}[i]$  and  $\sigma_{\text{sgn}(z_2)} = \text{sgn}(z_2)$  then
17        | |  $\vec{T}[i+1] \leftarrow \text{True}$ 
18        | |  $\vec{T}[i] \leftarrow \text{False}$ 
19        | |  $C \leftarrow C + 1$  // Transition to next state and increment counter C
20      | if  $\vec{T}[2]$  and  $\sigma_{\text{sgn}(z_2)} = \text{sgn}(z_2)$  then
21        | |  $C \leftarrow C + 1$  Confirm final state and increment counter
22        | | if  $C \geq C_{\max}$  then
23          | | | Robot Action: Stop Movement // Pause 0.1s before path switch
24          | | |  $C \leftarrow 0$  // Reset change counter for next change
25          | | |  $\vec{T} \leftarrow [False, False, False]$  // Reset transition states
26  if  $\sigma_{\text{sgn}(z_2)} \neq 0$  or  $C \geq C_{\max}$  then
27    | Robot Action: Continue or pivot to Red
28  else
29    | Robot Action: Continue or pivot to Blue
30  foreach  $(x_i, y_i) \in \{(x_i, y_i)\}_{i=1}^N$  do
31    | if  $x_{1b} \leq x_i \leq x_{2b} \wedge y_{1b} \leq y_i \leq y_{2b}$  or  $x_{1r} \leq x_i \leq x_{2r} \wedge y_{1r} \leq y_i \leq y_{2r}$  then
32    | | Robot Action: Stop Movement // If Human presses any buzzer, then stop and commit to the closest
33    | | | available option either Red or Blue.
34    | | Break: Exit
34  $\mathbf{p}_{\text{robot}}$ : Current Pose of the robot's end effector relative to camera frame.  $d_{\text{blue}} = \|\mathbf{p}_{\text{robot}} - \mathbf{p}_{\text{buzzer}}[\text{"blue"}][0]\|$ 
35  $d_{\text{red}} = \|\mathbf{p}_{\text{robot}} - \mathbf{p}_{\text{buzzer}}[\text{"red"}][0]\|$ 
36 if  $d_{\text{blue}} < d_{\text{red}}$  then
37 | Robot Action: Press Blue buzzer // Nearest buzzer is blue
38 else
39 | Robot Action: Press Red buzzer // Nearest buzzer is red

```

---

the robot towards the agreed convergence choice  $O$ . Upon detection of a hand coordinate within the bounding box of the red or blue buzzer, Algorithm 1 ceases the transmission of  $z_r$  and  $\{(x_i, y_i)\}_{i=1}^N$ , causing the robot to stop. The robot then commits to press the nearest buzzer, determined by its current end effector position.

## 5 HUMAN-IN-LOOP MANIPULATION VIA ROBOTIC EYE-GAZE

An experimental study [41] found that even during the human brain’s resting state—in the background—it still prepares and influences decision-making, even when not engaged with direct stimuli. This foundational activity was evident in trials 1-3 of our study, where despite the robotic eye gaze being neutral and offering no external cues, participants’ decisions were subtly shaped by their intrinsic brain activity. These internal biases served as initial conditions for human opinion formation. In contrast, during trials 4-8, the activation of the robotic eye gaze just before the onset of auditory cues (1, 2, 3, go) marked a shift to externally guided decision-making. Here, participants’ brain activity was more dynamically responsive to these immediate external stimuli rather than being predominantly influenced by the brain’s resting state, effectively mitigating internal bias. The presence of directed visual cues from the robotic eye shifted the cognitive processing from an internally guided to an externally responsive mode, aligning with findings that external stimuli can override internal predispositions in decision contexts.

Thus, in the initial trials, internal biases serve as the initial conditions for human opinion dynamics, which are subsequently updated by observing the robot’s behavior. This influence is demonstrated by changes in the intended human paths from one option to another, as shown in Section 6 and further discussed in Section 8. In later trials, where the robotic eye imparts an external bias, it mitigates these initial internal biases. Instead, the human brain may respond directly to what it observes, adhering to the non-linear opinion dynamics model described in Equation (2). Furthermore, since participants were not explicitly informed about the purpose and functioning of robotic eyes at any point before or during the experiment and had to deduce environmental cues on their own, this approach effectively prevented any preconceived or expected bias.

During the experiment, the robotic eyes executed specific movements across different iterations to draw participants’ attention to specific external stimuli. In the first three iterations, the robotic eyes remained in the center position, looking straight ahead at zero radians to establish a neutral baseline as shown in Figure 8(a).

In the 4<sup>th</sup> iteration, the robotic eyes performed a rapid and conspicuous movement to capture participants’ attention by setting the servo PWM values to their mechanical limits. First, the left eye’s yaw  $\psi_L$  and pitch  $\theta_L$ , along with the right eye’s yaw  $\psi_R$ , were set to 2000 microseconds, corresponding to 1.57 radians, towards the red buzzer. Moreover,  $\theta_R$  was adjusted for 1000 microseconds, having  $-0.52$  radians, adding a downward orientation. This dramatic setup was designed to maximize visual and auditory impact. Following this attention-seeking movement, the eyes shifted toward the blue buzzer, the designated convergence option  $O = \text{“blue”}$ , with both eyes shifting 150 pulse units in yaw and 100 in pitch. This repositioning set the yaw  $\psi_L, \psi_R$  to  $-0.47$  radians and the pitch  $\theta_L, \theta_R$  to 0.31 radians, slightly downward as shown in Figure 8(b).

In the 5<sup>th</sup> iteration, robotic eyes were adjusted to significantly enhance their visibility. The servos moved 170 pulse units for yaw and pitch, reaching approximately  $+0.53$  radians in yaw toward red and  $-0.53$  radians in pitch downward. Starting from the 5<sup>th</sup> trial, the common convergence option  $O$  was switched from “blue” to “red” to counteract participants’ expectancy bias toward the blue option from the 4<sup>th</sup> trial. This modification was intended to challenge participants’ possible expectations that the gaze would remain on the blue buzzer. By altering the gaze direction in this trial, the experiment sought to assess whether participants would recalibrate their expectations and decision-making processes when faced with inconsistent cues, thereby mitigating the influence of prior experiences on their current

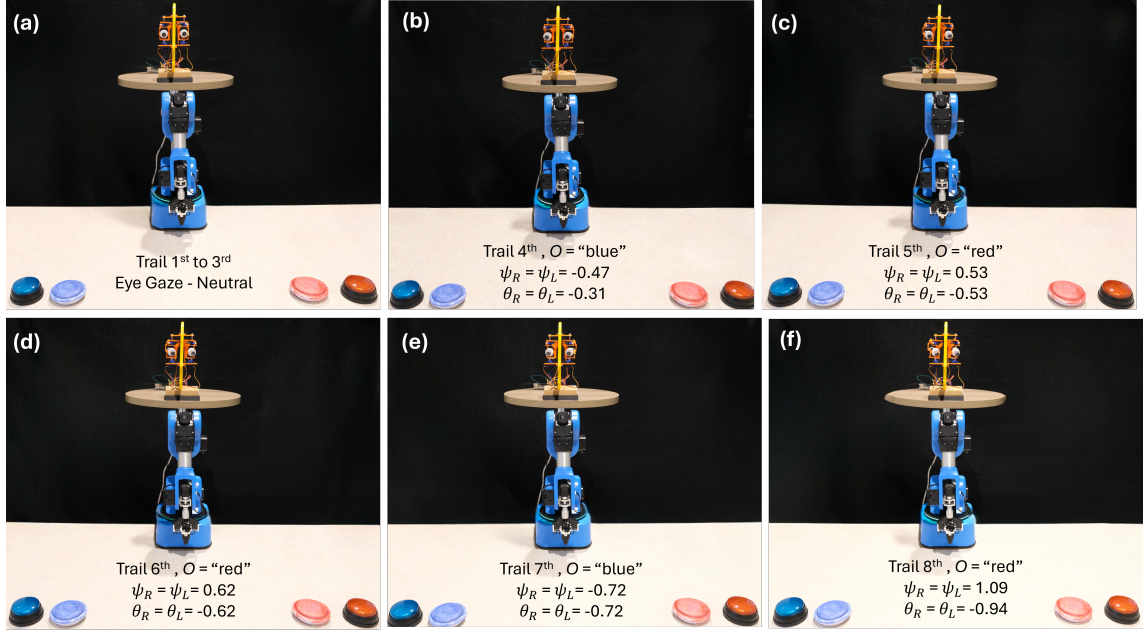


Fig. 8. Illustration of the human participant’s view of the robotic eye gaze, robotic arm, and buzzer across different trials. (a) In trials 1 to 3, the robot remains neutral, consistently selecting the opposite buzzer color to demonstrate disagreement. (b) In trial 4, the robotic eye gaze is directed towards the blue buzzer, signaling a shift towards alignment. (c) In trial 5, the robot intensifies its gaze towards the red buzzer (d) In trial 6, the gaze remains fixed on the red buzzer (e) In trial 7, the gaze returns to the blue buzzer (f) In trial 8, the robotic eye gaze intensifies towards the red buzzer, marking the final and most pronounced visual clues. From trials 4 to 8, the robot progressively strengthens its gaze towards the selected option, influencing the human’s decision-making process.

perceptions and choices. During 6<sup>th</sup> iteration, the robotic eyes were adjusted by moving 200 pulse units in both yaw and pitch. These movements correspond to approximately  $+0.62$  radians in yaw towards red and a similar change in pitch of  $-0.62$  radians downwards. This adjustment aimed to enhance the visual prominence of the robotic gaze, focusing participants on adapting to visual cues for decision-making rather than pattern decoding.

In the 7<sup>th</sup> iteration, the robotic eyes shifted 230 pulse units in both yaw and pitch toward the blue buzzer, positioning at  $-0.72$  radians in yaw and  $0.72$  radians downward in pitch, effectively redirecting attention. In the 8<sup>th</sup> iteration, the eyes moved 350 pulse units toward the red buzzer and 300 units downward, translating to  $+1.09$  radians in yaw and  $-0.94$  radians in pitch, achieving the most pronounced gaze to influence participant decision-making.

## 6 EXPERIMENTAL DEMONSTRATIONS

In our human-robot interaction experiment for decision-making involving a diverse cohort of 51 human participants ( $N=51$ ), Algorithms 1 and 2, described in Section 5, underwent extensive testing to rigorously assess their robustness and ensure consistent, reproducible optimal outcomes. Figure 9 illustrates participant interactions during the first three disagreement trials using the non-linear opinion dynamics model parameters from Table 1. In these trials, Algorithm 2 ensured that the robot consistently selected a buzzer color contrary to the participant’s initial choice. Figure 9(a) illustrates the interaction dynamics during the first trial of the 32<sup>nd</sup> participant. Initially inclined to press the red buzzer, the participant updated their opinion ( $z_t$ ) to align with the robot’s intended choice after observing it moving toward the



blue buzzer at  $t = 3.7$  seconds. Simultaneously, operating under Algorithm 1, the robot proactively altered its trajectory following the directives of Algorithm 2. The distance  $d$  decreased progressively as the human neared a decision, and the angle  $\theta$  was adjusted accordingly to reflect the human’s updated opinion. An accompanying plot of the human hand trajectory highlights the mid-interaction modification of human opinion.

At the beginning of the experiment, all participants were instructed that they were allowed a single alteration in their path before crossing the black decision commit line to match the robot’s choice. Any violation of this rule would result in a one-point penalty deducted from the participant’s overall score. Despite these guidelines, some participants changed their paths multiple times in efforts to align their choices with those of the robot, thereby attempting to maximize their scores. Figure 9(b) illustrates 32<sup>nd</sup> participant in 3<sup>rd</sup> trial after experiencing repeated disagreements from the robot in first two trials. Initially heading towards the blue buzzer, the participant switched to red, then reverted to blue, and made a last-minute attempt to switch back to red upon observing the robot’s movement. However, upon the realization that he had already crossed the decision commit line, he ultimately reverted and committed to blue. This scenario demonstrates the robot’s deceptive behavior capability, driven by Algorithm 2, alongside its ability to rapidly form reliable disagreeing opinions using non-linear opinion dynamics. The robot adapts to multiple directional changes in response to varying human opinions and actively counters human actions with multiple switches.

Figure 9 (c) illustrates the 47<sup>extth</sup> participant in the 3<sup>extrd</sup> trial, with the robot configured for disagreement. Having previously faced two trials of deliberate opposition from the robot, the participant anticipated further adversarial robot behavior. In response, the participant initiated an early strategic switch at the start of the interaction. However, the robot’s swift and adaptive opinion modifications, enabled by Algorithm 1, allowed it to quickly adjust its responses to continue its disagreement. This scenario effectively simulates real-world conditions in which continuous disagreement necessitates adaptive collaboration methods. These trials underscore the need for advanced collaborative mechanisms, leading to the deployment of the robotic eye gaze and bias control algorithms as facilitators for achieving consensus between human and robot decisions.

Figure 10(a) displays 35<sup>th</sup> participant in the 7<sup>th</sup> trial, where the robotic eye was activated prior to the interaction, directing its gaze towards the blue buzzer, as shown in Figure 8(e). The bias control algorithm within Algorithm 1 was activated, with the non-linear robot opinion, bias dynamics, and human opinion observation parameters set according to Table 1. With the input  $O = \textit{“blue”}$ , the robot’s opinion was directed toward the blue buzzer, increasing its bias toward this selection. The bias plot in Figure 10(a) indicates that once the robot’s bias ( $b_r$ ) exceeded the critical threshold, signifying social attention to human opinion, it consistently maintained this bias toward the blue option for the rest of the interaction. Meanwhile, the human’s internal opinion dynamics were influenced by the bias imparted from the robot’s eye gaze, compelling the participant to firmly press the blue buzzer without any deviations in hand trajectory. In the 8th and final trial of the same 35<sup>th</sup> participant, the robotic eye was oriented toward the red buzzer, with Algorithm 2 configured for the input  $O = \textit{“red”}$ . This final interaction, shown in Figure 10(b), demonstrated the most pronounced effects of eye gaze and recorded the shortest time to consensus among all trials. This outcome illustrates that as participants internalize the external stimulus or bias from the robotic eye—and as the robot consistently aligns with the same buzzer color—their trust in the robotic guidance intensifies, leading to a quicker consensus.

Although most trials configured for disagreement resulted in dissensus, there were instances where quick, strategic end-moment switches enabled some participants to align their choices with the robot’s final choices during the initial trial. However, almost all participants encountered at least one instance of disagreement, which motivated them to actively observe the environment for guidance cues from the robotic eye gaze, thereby facilitating collaboration. Furthermore, in the early rounds, when the robotic eye was activated, participants—driven by growing trust in the

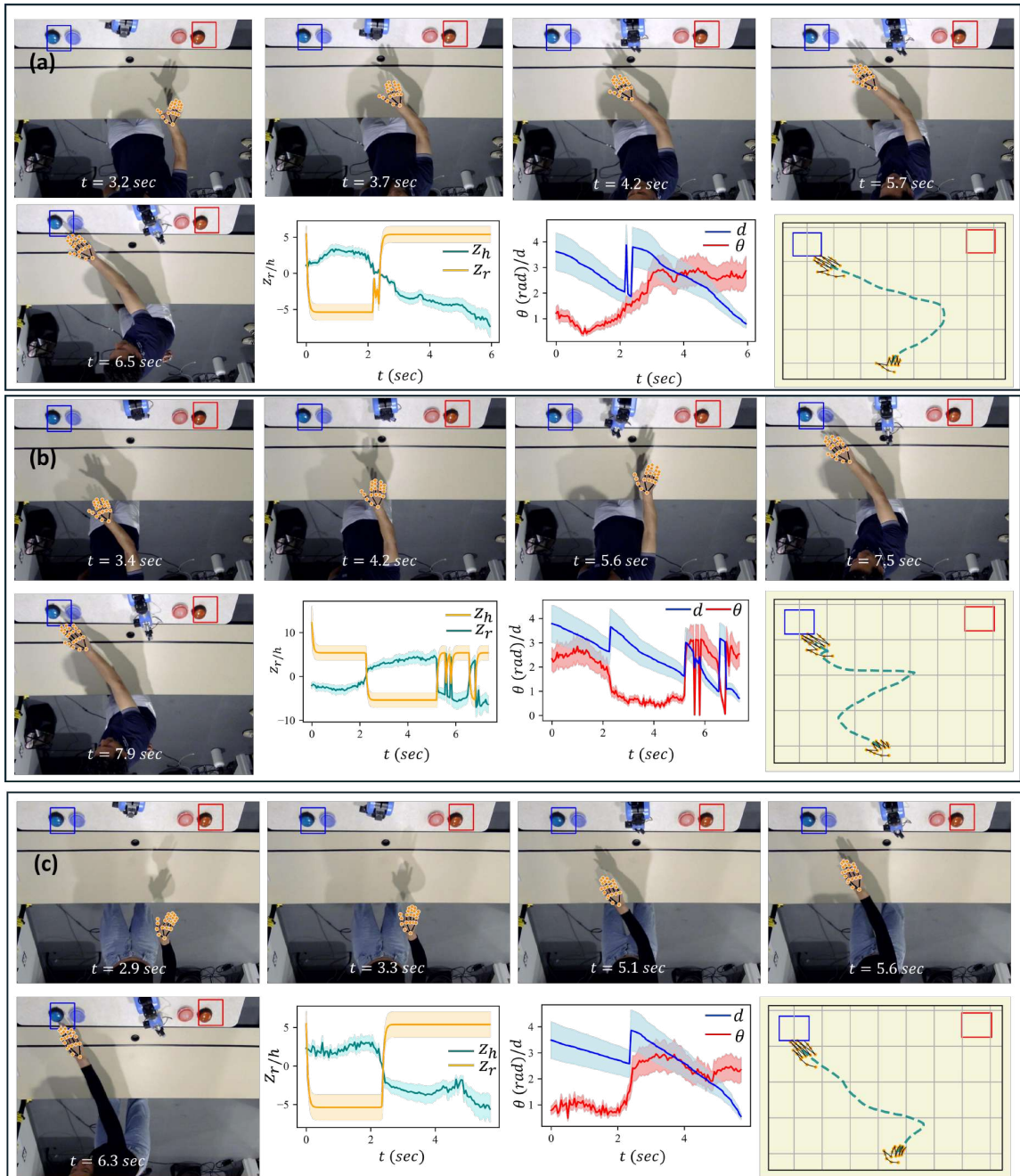


Fig. 9. Experimental illustration of mid-switch, multiple switches, and strategic early switch by human participants in trials 1 to 3, where the robot is configured to show disagreement.

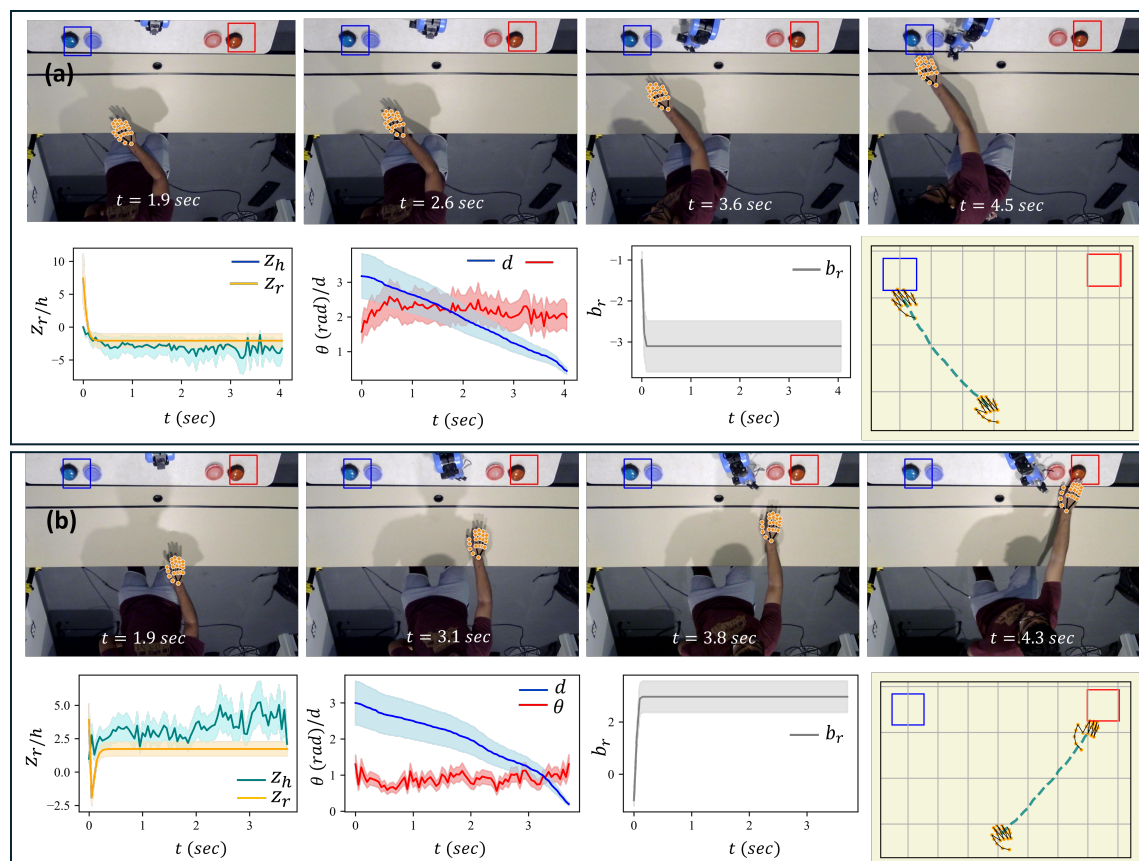


Fig. 10. Illustration of trials 9 and 10, where the robotic eye is activated to provide visual cues to the human participant, showing no adjustment in hand path trajectory and a direct consensus between human and robot actions as well as opinions.

robot’s behavior—adjusted their hand paths to align with the robot’s choices. The progression of these switches across the interaction trials is thoroughly discussed in Section 7, which presents the comprehensive results of all experiments and the overall trends.

## 7 OVERALL EXPERIMENTAL OUTCOMES and TREND

We categorized the decision-making behavior of the participants into four distinct types. Agreement (A) without path alterations, Direct Disagreement (D) also without path alterations, Change to Agreement (CA) involving a single opinion modification, and Change to Disagreement (CD). Figure 11(a) illustrates the dynamics of these decision-making behaviors across all eight experimental trials. Notably, when the robot was configured to initiate interactions with a stance of disagreement, a predominant selection of ‘D’ (*Direct Disagreement*) was observed experimentally during the initial trials (1<sup>st</sup> to 3<sup>rd</sup>), simulating a prevalent initial dissensus between human participants and the robot. A subset of participants strategically outmaneuvered the robot by adeptly modifying their hand trajectories—either spontaneously or at critical junctures—to transition into ‘A’ (*Agreement*) or ‘CA’ (*Change to Agreement*). However, instances of ‘CD’

(Change to Disagreement) were exceptionally rare, indicating that participants were highly motivated and focused on achieving the highest possible score.

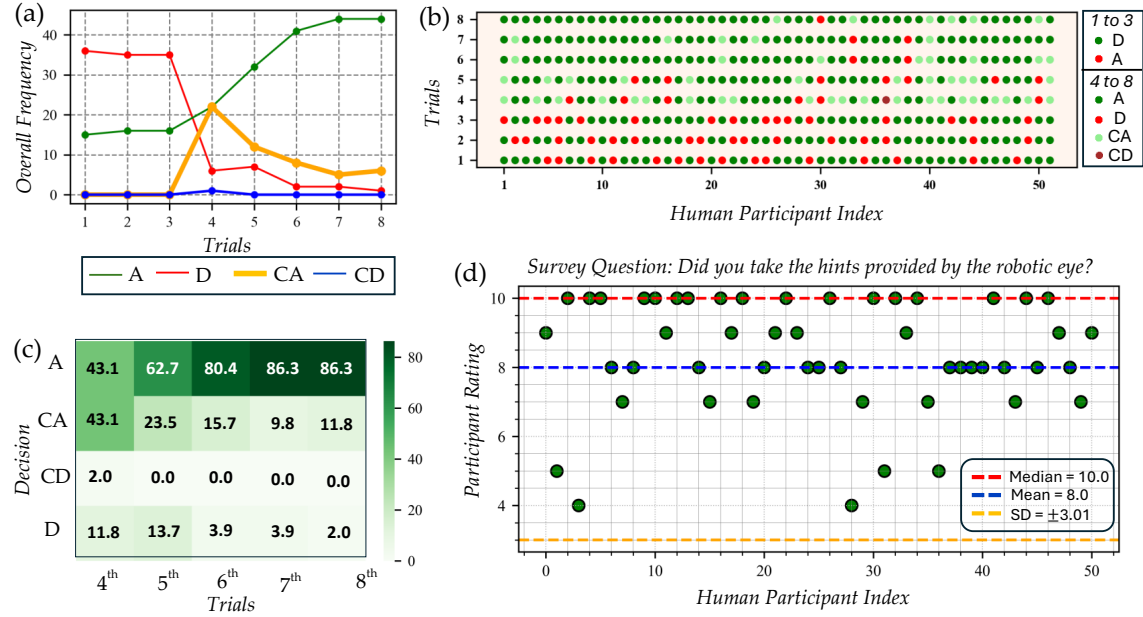


Fig. 11. Experimental outcomes illustrating: (a) Line plot showing the relationship between trial number and overall frequency of A (Direct Agreement), D (Direct Disagreement), CA (Change to Agreement), and CD (Change to Disagreement); (b) Overall scatter plot representing all human participants and their corresponding choices across 8 trials; (c) Heat map displaying participant choices from the 4<sup>th</sup> to 8<sup>th</sup> trials; (d) Scatter plot with mean, median, and standard deviation of participants' ratings in response to the question 'Did you take the hints provided by the robotic eye?' on a scale of 1 to 10.

To analyze the overall trends after the 3<sup>rd</sup> trial, we examined both Figure 11(a) and the heatmap of participants' decisions from the 4<sup>th</sup> to 8<sup>th</sup> trials, as shown in Figure 11(c). It is evident that as the visual cues from robotic eye gaze became increasingly pronounced from the 4<sup>th</sup> to 8<sup>th</sup> trial, the behavior of Direct Agreement (A) was predominantly adopted, and Disagreement (D) decreased gradually. This suggests that visual cues from the robot's eyes can effectively build consensus between humans and the robot by imparting bias as an external stimulus in human opinion dynamics. Notably, a spike in Change to Agreement (CA) occurred during the 4<sup>th</sup> trial, correlating with the robot's abrupt transition from a stance of disagreement to bias assimilation without subsequent deviations or disputes. This abrupt behavioral shift prompted participants to closely examine the cues of the robotic eye, assessing whether the robot consistently followed these visual signals when selecting the corresponding buzzer. Furthermore, the participants were not previously briefed about the function and purpose of the robotic eye. Its initial activation, coupled with the mechanical sounds emitted by the servos, prompted participants to infer its intent and operational significance. Analysis of the heatmap and line graph in Figures 11(a) and 11(c) further demonstrates a progressive decline in Change to Agreement (CA) as the trials advanced, culminating in an increased prevalence of Direct Agreement (A). This progression demonstrates a gradual increase in participants' trust in the visual guidance of the robotic eye over successive trials.

Figure 11(b) presents the comprehensive data from the experiment with 51 participants across all trials. Hypothetically, assuming perfect disagreement in the initial three trials—with participants strictly adhering to the experimental protocol

without making last-minute changes or quick switches—and assuming hypothetical agents (human participants) fully trusted the robotic eye cues from the 4<sup>th</sup> to 8<sup>th</sup> trials, the scatter plot should predominantly show all green points, indicating disagreement initially and agreement subsequently. Contrary to expectations, the unpredictability of irrational human behavior led to significant deviations. Red points highlight unexpected agreements in the initial trials and disagreements in the later ones. Each participant only exhibited a change to agreement behavior starting from the 4<sup>th</sup> trial, which gradually diminished, transitioning to complete agreement by the 8<sup>th</sup> iteration. The majority of the 51 participants reached a consensus in the last five trials, with only a few outliers. The potential reasons for these outliers, including participants’ educational backgrounds, are discussed in Section 8, “User Feedback Analysis.”

A statistical analysis of the post-experiment survey responses to the question, “Did you take the hints provided by the robotic eye?”—rated by all participants on a scale from 0 (not at all) to 10 (heavily)—revealed a median score of 10 and a mean of 8, as shown in Figure 11(d). These results underscore the significant role of human trust in the robotic eye’s visual cues, as the majority of participants integrated these cues into their decision-making processes. By synthesizing these survey results with the observed decision-making behavior during the experiment, we affirm the answer to Research Question 1 (RQ1): Yes, Bias or external stimuli can be deliberately introduced into human decision-making as a psychological factor to effectively facilitate consensus during human-robot interactions.

Addressing Research Question 2 (RQ2): Once humans assimilate their opinions with the bias imparted by visual cues from the robotic eye, they initially test the validity and efficacy of the provided guidance. If the results align with their expectations, they gradually increase their trust levels, marking a significant evolution in human-robot interactions. This increased trust leads them to rely on this guidance to maintain smooth collaboration and fulfill personal objectives (such as achieving high scores in our experiments).

A marked increase in agreement immediately following the activation of the robotic eye, along with the scarcity of shifts to disagreement, addresses Research Question 3 (RQ3): Persistent early disagreements motivate humans to align their choices with those of the robot when mediated by visual cues as an external biasing factor. Furthermore, the robust performance of Algorithms 1 and 2, as demonstrated in Section 7 and subsequent analyses, confirms that utilizing non-linear opinion dynamics—without dynamic bias for disagreement and with bias for consensus-building—can model safe and efficient real-time robot decisions during interactions with humans. Non-linear opinion dynamics with dynamic bias control effectively manage controlled consensus and dissensus in response to human actions, providing a tractable mathematical and numerical analysis, thereby addressing Research Question 4 (RQ4).

## 8 USER FEEDBACK ANALYSIS

Based on post-experiment feedback and interviews, we aim to validate the following hypotheses. These hypotheses will guide future tweaks to our algorithms and experimental settings, incorporating the insights gained. With respect to participants’ demographic backgrounds, we postulate **Hypothesis 1 (H1)** as follows:

**Hypothesis 1 (H1):** The age and gender of participants will not significantly influence their overall scores in the experiment.

The statical analysis, depicted in Figure 12(a), conducted using the Ordinary Least Squares (OLS) method, assessed the impact of age and gender on participants’ overall scores. The analysis yielded an  $R^2$  value of 0.098, indicating that these predictors account for only 9.8% of the variance in scores. The model’s F-statistic is 2.606, with a p-value of 0.0843, suggesting the results do not reach conventional significance levels ( $p < 0.05$ ).

The regression analysis delineated distinct impacts from the examined predictors on game scores. Specifically, age demonstrated a minor but statistically significant adverse effect, with each additional year decreasing the score by

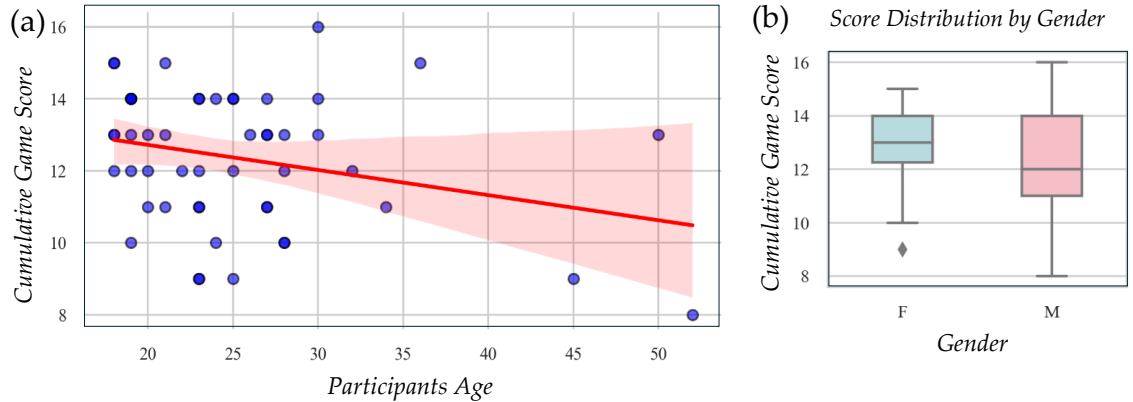


Fig. 12. Analysis of participants' feedback showing: (a) Regression plot between participant age and their cumulative game score; (b) Box plot displaying score distribution by gender.

approximately 0.0781 points, evidenced by a regression coefficient of  $-0.0781$  ( $p$ -value = 0.032). This finding suggests that age-related factors may influence game performance, with older participants tending to score lower than the younger participants. In contrast, Figure 12(b) shows that gender did not have a significant effect on game scores, as indicated by a coefficient of  $-0.5872$  ( $p$ -value = 0.302). Consequently, the data support the hypothesis that gender does not significantly impact scores, validating this aspect of our initial hypothesis. However, the hypothesis concerning age is not supported, as the analysis confirms a significant correlation between age and performance. This lack of significance supports the hypothesis that gender does not substantially influence game scores, thus confirming the hypothesis partially for gender but not for age.

The significant influence of age on interaction scores within human-robot interactions underscores the necessity for age-adaptive technologies. These adaptations are crucial for enhancing engagement and operational efficiency, especially for elderly users of robotic technology. In contrast, the absence of significant gender effects supports the advancement of gender-neutral robotic designs, ensuring equitable usability for all users.

To investigate the visual anthropomorphism capabilities of the robotic eye design, we formulated **Hypothesis 2 (H2)** as follows:

**Hypothesis 2 (H2):** The majority of participants will recognize the robotic eye through visual observation alone, without any prior explicit information about it.

In the post-experimental feedback survey, participants were asked, "Did you notice the robotic eyes in the environment after a few trials?" They rated their noticeability on a scale from 1 (Not at all) to 10 (Highly). To support **Hypothesis 2**, we set a threshold that 80% of participants must rate their recognition at seven or higher. As shown in Figure 13(a), approximately 84.31% of participants provided ratings above this threshold, validating **Hypothesis 2 (H2)**. These results substantiate that the robotic eyes function effectively as an anthropomorphic mechanism, enhancing human-robot collaboration. Consequently, the design of robotic eyes indeed influences human interaction toward a specific collaborative outcome. This answers our research question 5 (RQ5): Yes, the presented design of robotic eyes serve as an effective anthropomorphic mechanism to guide humans towards a specific collaborative option with the robot.

From the post-experiment interviews, it was observed that participants from computer science or robotics backgrounds predominantly perceived the robotic eyes as camera sensors intended to detect their actions, even though the robotic

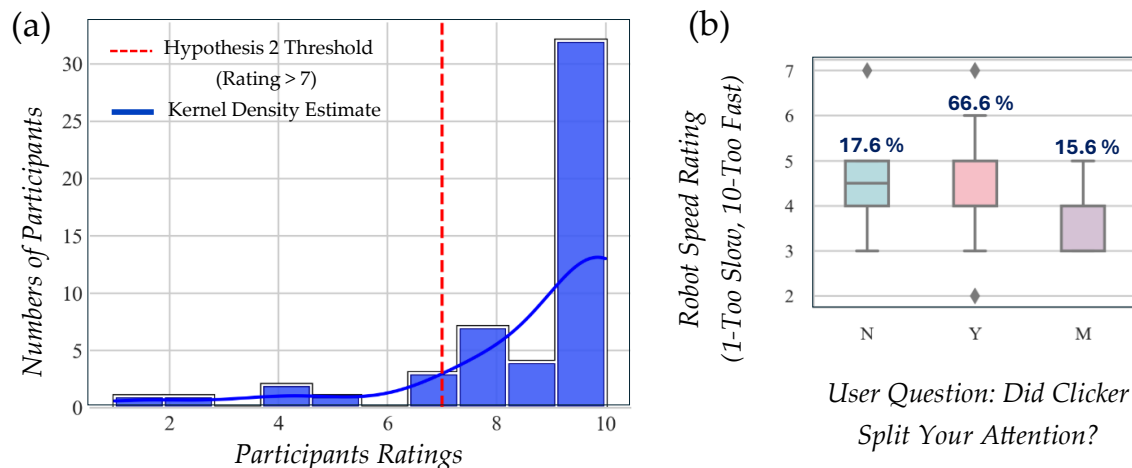


Fig. 13. (a) Participants' ratings on a 1 to 10 scale versus the number of participants for the post-experiment feedback survey question: 'Did you notice the robotic eyes in the environment after a few trials?'; (b) Box plots of participants' feedback ratings on a scale of 1 to 10 in response to the question: 'Did the clicker split your attention or slow you down during interaction and decision-making?'.

eyes lacked any camera functionality and were designed to guide participants' decisions toward consensus with the robot. In contrast, participants with general engineering backgrounds often interpreted robotic eyes as mechanisms intended to confuse them and negatively affect their scores, a perception potentially influenced by the initial three trials configured for disagreement. In contrast, participants from non-technical backgrounds, such as maintenance workers, typically viewed the robotic eyes as a straightforward visual guidance source, enabling effective collaboration with the robot without forming any misconceptions.

Now, to investigate the effect of cognitive load on decision-making, the following **Hypothesis 2 (H2)** was postulated as follows:

**Hypothesis 3 (H3):** Participants who reported that using the clicker behind their back caused them to split their attention would perceive the speed of the robotic arm differently compared to those answering 'No' or 'Maybe'.

Surprisingly, the data from Figure 13(b) reveal that 66.6% of participants felt that the clicker caused attention splitting, slowing their hand motion. However, an ANOVA test with an F-statistic of 1.04 and a p-value of 0.3602 showed no significant differences in arm speed ratings among the groups, leading to the retention of the null hypothesis and suggesting uniform perceptions across the groups. This outcome does not support **Hypothesis 3**, indicating that the cognitive load imposed by the clicker did not affect the participants' perceptions of the robotic arm's speed. This suggests that while cognitive load can slow down physical response, it does not alter perceptions of the robot's performance, leading to strategic considerations for future human-robot interaction design involving cognitive load.

Overall, the experimental data indicate that while cognitive load and age significantly affect participants' responses and performance, gender does not have a measurable impact. These findings are significant because they underscore the importance of accommodating age differences and managing cognitive load in human-robot interaction design. In addition, the design of robotic eyes effectively fosters anthropomorphism, enhancing human-robot collaboration. This further highlights the efficacy of anthropomorphic cues in improving interaction outcomes.

## 9 CONCLUSION, LIMITATIONS and FUTURE WORK

This article demonstrated how effective and gradual collaboration between humans and robots can be facilitated using bias or external stimuli by modeling human and robot opinions through non-linear opinion dynamics. Our experimental results, including controlled consensus and dissensus outcomes, participant feedback, and post-experiment analysis, confirm that biases in the form of visual cues from robotic eyes can effectively transition interactions from dissensus to consensus. Additionally, for our experimental setup with optimized non-linear opinion dynamics parameters, we present a detailed numerical analysis, including parameter sweeping, determination of the number of opinion equilibrium solutions, and continuation analysis of unique equilibria to explore the dynamics of growing bias during interactions. The dynamic bias model emphasizes that the bias with which humans and robots engage must surpass their respective social attentions to achieve consensus.

The current bias-controlled non-linear opinion dynamics model has limitations regarding how it captures the divergence between human internal and external opinions, known as implicit and explicit opinions [63]. These divergences can lead to discrepancies between physical actions, influenced by social pressures and internal beliefs. Furthermore, the model does not currently incorporate a mathematical representation of trust [26]. Future enhancements will address these gaps by integrating implicit and explicit opinions and quantifying the trust factor.

In the future, we aim to develop models that more accurately reflect human opinion dynamics in real-world scenarios, examining how bias dynamics affect opinion and trust dynamics. Additionally, future work will also focus on developing a control algorithm for robot behavior that accounts for these complexities in human decision-making. Future experimental work will extend to uncontrolled environments such as factories and warehouses, where workers are engaged in daily maintenance tasks in collaboration with robots.

## References

- [1] [n. d.]. Ned2 – 6 axis desktop collaborative arm-robot. <https://niry.com/product/6-axis-robotic-arm/>. Accessed: 2024-10-14.
- [2] Giovanna Amorim, Maria Santos, Shinkyu Park, Alessio Franci, and Naomi Ehrich Leonard. 2024. Threshold Decision-Making Dynamics Adaptive to Physical Constraints and Changing Environment. In *2024 European Control Conference (ECC)*. IEEE, 1908–1913. <https://doi.org/10.23919/ECC64448.2024.10591177>
- [3] Chris L. Baker and Joshua B. Tenenbaum. 2014. Modeling Human Plan Recognition Using Bayesian Theory of Mind. In *Plan, Activity, and Intent Recognition*, Gita Sukthankar, Christopher Geib, Hung Hai Bui, David V. Pynadath, and Robert P. Goldman (Eds.). Morgan Kaufmann, Boston, 177–204. <https://doi.org/10.1016/B978-0-12-398532-3.00007-5>
- [4] Marwen Belkaid, Kyveli Kompatsiari, Davide De Tommaso, Ingrid Zablith, and Agnieszka Wykowska. 2021. Mutual gaze with a robot affects human neural activity and delays decision-making processes. *Science Robotics* 6, 58 (2021), eabc5044. <https://doi.org/10.1126/scirobotics.abc5044>
- [5] Anastasia Bizyaeva, Alessio Franci, and Naomi Ehrich Leonard. 2023. Nonlinear Opinion Dynamics With Tunable Sensitivity. *IEEE Trans. Automat. Control* 68, 3 (2023), 1415–1430. <https://doi.org/10.1109/TAC.2022.3159527>
- [6] Anastasia Bizyaeva, Timothy Sorochkin, Alessio Franci, and Naomi Ehrich Leonard. 2021. Control of Agreement and Disagreement Cascades with Distributed Inputs. In *2021 60th IEEE Conference on Decision and Control (CDC)*. IEEE, 4994–4999. <https://doi.org/10.1109/CDC45484.2021.9683650>
- [7] Jean-David Boucher, Ugo Pattacini, Amelie Lelong, Gerard Bailly, Frederic Elisei, Sascha Fagel, Peter F. Dominey, and Jocelyne Ventre-Dominey. 2012. I Reach Faster When I See You Look: Gaze Effects in Human–Human and Human–Robot Face-to-Face Cooperation. *Frontiers in Neurobotics* 6 (2012). <https://doi.org/10.3389/fnbot.2012.00003>
- [8] Cynthia Breazeal. 2002. Regulation and Entrainment in Human–Robot Interaction. *The International Journal of Robotics Research* 21, 10-11 (2002), 883–902. <https://doi.org/10.1177/0278364902021010096>
- [9] Cynthia Lynn Breazeal and Paul M. Fitzpatrick. 2000. That Certain Look: Social Amplification of Animate Vision. <https://api.semanticscholar.org/CorpusID:17369026>
- [10] Charlotte Cathcart, Maria Santos, Shinkyu Park, and Naomi Ehrich Leonard. 2023. Proactive Opinion-Driven Robot Navigation Around Human Movers. In *Proceedings of the 2023 IEEE/RSJ International Conference on Intelligent Robots and Systems (IROS)*. 4052–4058. <https://doi.org/10.1109/IROS55552.2023.10341745>
- [11] Boyuan Chen, Carl Vondrick, and Hod Lipson. 2021. Visual behavior modelling for robotic theory of mind. *Scientific Reports* 11, 1 (2021), 424. <https://doi.org/10.1038/s41598-020-77918-x>



- [12] Paul Churchland and John Haldane. 1988. Folk Psychology and the Explanation of Human Behaviour. *Proceedings of the Aristotelian Society, Supplementary Volumes* 62 (1988), 209–254. <http://www.jstor.org/stable/4106765>
- [13] Kourosh Darvish, Enrico Simetti, Fulvio Mastrogiovanni, and Giuseppe Casalino. 2021. A Hierarchical Architecture for Human–Robot Cooperation Processes. *IEEE Transactions on Robotics* 37, 2 (2021), 567–586. <https://doi.org/10.1109/TRO.2020.3033715>
- [14] V. M. Eguiluz, N. Masuda, and J. Fernández-Gracia. 2015. Bayesian Decision Making in Human Collectives with Binary Choices. *PLoS ONE* 10, 4 (2015), e0121332. <https://doi.org/10.1371/journal.pone.0121332>
- [15] Connor Esterwood and Lionel P. Robert. 2023. The theory of mind and human–robot trust repair. *Scientific Reports* 13, 1 (2023), 9877. <https://doi.org/10.1038/s41598-023-37032-0>
- [16] A. F. Filippov. 1988. *Differential Equations with Discontinuous Righthand Sides: Control Systems*. Mathematics and its Applications, Vol. 18. Springer Dordrecht. <https://doi.org/10.1007/978-94-015-7793-9>
- [17] Matan Fintz, Margarita Osadchy, and Uri Hertz. 2022. Using deep learning to predict human decisions and using cognitive models to explain deep learning models. *Scientific Reports* 12, 1 (2022), 4736. <https://doi.org/10.1038/s41598-022-08863-0>
- [18] Samuel J. Gershman. 2017. Correction: A Unifying Probabilistic View of Associative Learning. *PLOS Computational Biology* 13, 11 (2017), e1005829. <https://doi.org/10.1371/journal.pcbi.1005829>
- [19] S. Grushko, A. Vysocký, P. Ošćádal, M. Vocetka, P. Novák, and Z. Bobovský. 2021. Improved Mutual Understanding for Human-Robot Collaboration: Combining Human-Aware Motion Planning with Haptic Feedback Devices for Communicating Planned Trajectory. *Sensors* 21, 11 (2021). <https://doi.org/10.3390/s21113673>
- [20] Soheil Habibian, Antonio Alvarez Valdivia, Laura H. Blumenschein, and Dylan P. Losey. 2023. A review of communicating robot learning during human-robot interaction. *arXiv preprint arXiv:2312.00948* (2023). <https://arxiv.org/abs/2312.00948>
- [21] Mehdi Hellou, Samuele Vinanzi, and Angelo Cangelosi. 2023. Bayesian Theory of Mind for False Belief Understanding in Human-Robot Interaction. In *Proceedings of the 2023 32nd IEEE International Conference on Robot and Human Interactive Communication (RO-MAN)*. 1893–1900. <https://doi.org/10.1109/RO-MAN57019.2023.10309356>
- [22] Laura M. Hiatt, Cody Narber, Esube Bekele, Sangeet S. Khemlani, and J. Gregory Trafton. 2017. Human modeling for human–robot collaboration. *The International Journal of Robotics Research* 36, 5-7 (2017), 580–596. <https://doi.org/10.1177/0278364917690592>
- [23] Pierce Howell, Jack Kolb, Yifan Liu, and Harish Ravichandar. 2023. The Effects of Robot Motion on Comfort Dynamics of Novice Users in Close-Proximity Human-Robot Interaction. In *Proceedings of the 2023 IEEE/RSJ International Conference on Intelligent Robots and Systems (IROS)*. 9859–9864. <https://doi.org/10.1109/IROS55552.2023.10341487>
- [24] Jie Huang, Wenhua Wu, Zhenyi Zhang, and Yutao Chen. 2020. A Human Decision-Making Behavior Model for Human-Robot Interaction in Multi-Robot Systems. *IEEE Access* 8 (2020), 197853–197862. <https://doi.org/10.1109/ACCESS.2020.3035348>
- [25] Yidi Huang, Qi Wei, Joseph L Demer, and Ningshi Yao. 2023. See What a Strabismus Patient Sees Using Eye Robots. In *2023 IEEE/RSJ International Conference on Intelligent Robots and Systems (IROS)*. IEEE, 4627–4632.
- [26] Bo Jiang, Yiyi Zhao, Jianglin Dong, and Jiangping Hu. 2024. Analysis of the influence of trust in opposing opinions: An inclusiveness-degree based Signed Defluant–Weisbush model. *Information Fusion* 104 (2024), 102173. <https://doi.org/10.1016/j.inffus.2023.102173>
- [27] Jeff Johnson. 2021. Human Decision-Making is Rarely Rational. In *Designing with the Mind in Mind (Third Edition)* (third edition ed.), Jeff Johnson (Ed.). Morgan Kaufmann, 203–223. <https://doi.org/10.1016/B978-0-12-818202-4.00012-X>
- [28] Daniel Kahneman and Amos Tversky. 2024. *Prospect Theory: An Analysis of Decision Under Risk*. Chapter 6, 99–127. [https://doi.org/10.1142/9789814417358\\_0006](https://doi.org/10.1142/9789814417358_0006)
- [29] Udo Kannengiesser and John S. Gero. 2019. Design thinking, fast and slow: A framework for Kahneman’s dual-system theory in design. *Design Science* 5 (2019), e10. <https://doi.org/10.1017/dsj.2019.9>
- [30] Tobias Kaupp, Alexei Makarenko, and Hugh Durrant-Whyte. 2010. Human–robot communication for collaborative decision making – A probabilistic approach. *Robotics and Autonomous Systems* 58, 5 (2010), 444–456. <https://doi.org/10.1016/j.robot.2010.02.003>
- [31] Koosha Khalvati, Seongmin A. Park, Saghar Mirbagheri, Remi Philippe, Mariateresa Sestito, Jean-Claude Dreher, and Rajesh P. N. Rao. 2019. Modeling other minds: Bayesian inference explains human choices in group decision-making. *Science Advances* 5, 11 (2019), eaax8783. <https://doi.org/10.1126/sciadv.aax8783>
- [32] Helena Kiilavuori, Veikko Sariola, Mikko J. Peltola, and Jari K. Hietanen. 2021. Making eye contact with a robot: Psychophysiological responses to eye contact with a human and with a humanoid robot. *Biological Psychology* 158 (2021), 107989. <https://doi.org/10.1016/j.biopsycho.2020.107989>
- [33] Choong Nyoung Kim, Kyung Hoon Yang, and Jaekyung Kim. 2008. Human decision-making behavior and modeling effects. *Decision Support Systems* 45, 3 (2008), 517–527. <https://doi.org/10.1016/j.dss.2007.06.011>
- [34] Minae Kwon, Erdem Biyik, Aditi Talati, Karan Bhasin, Dylan P. Losey, and Dorsa Sadigh. 2020. When Humans Aren’t Optimal: Robots that Collaborate with Risk-Aware Humans. In *Proceedings of the 2020 ACM/IEEE International Conference on Human-Robot Interaction*. 43–52. <https://doi.org/10.1145/3319502.3374832>
- [35] Naomi Ehrich Leonard, Anastasia Bizyaeva, and Alessio Franci. 2024. Fast and Flexible Multiagent Decision-Making. *Annual Review of Control, Robotics, and Autonomous Systems* 7 (2024), 19–45. <https://doi.org/10.1146/annurev-control-090523-100059>
- [36] Ji-An Li, Daoyi Dong, Zhengde Wei, Ying Liu, Yu Pan, Franco Nori, and Xiaochu Zhang. 2020. Quantum reinforcement learning during human decision-making. *Nature Human Behaviour* 4, 3 (2020), 294–307. <https://doi.org/10.1038/s41562-019-0804-2>

- [37] Shufei Li, Yingchao You, Pai Zheng, Xi Vincent Wang, and Lihui Wang. 2024. Mutual-cognition for proactive human–robot collaboration: A mixed reality-enabled visual reasoning-based method. *IJSE Transactions* 56, 10 (2024), 1099–1111. <https://doi.org/10.1080/24725854.2024.2313647>
- [38] Dylan P. Losey, Andrea Bajcsy, Marcia K. O’Malley, and Anca D. Dragan. 2022. Physical interaction as communication: Learning robot objectives online from human corrections. *The International Journal of Robotics Research* 41, 1 (2022), 20–44. <https://doi.org/10.1177/02783649211050958>
- [39] Ralph R. Miller, Robert C. Barnet, and Nicholas J. Grahame. 1995. Assessment of the Rescorla-Wagner model. *Psychological Bulletin* 117, 3 (1995), 363–386. <https://doi.org/10.1037/0033-2909.117.3.363>
- [40] Ashena Gorgan Mohammadi and Mohammad Ganjtabesh. 2024. On computational models of theory of mind and the imitative reinforcement learning in spiking neural networks. *Scientific Reports* 14, 1 (2024), 1945. <https://doi.org/10.1038/s41598-024-52299-7>
- [41] Takashi Nakao, Yu Bai, Hitomi Nashiwa, and Georg Northoff. 2013. Resting-state EEG power predicts conflict-related brain activity in internally guided but not in externally guided decision-making. *NeuroImage* 66 (2013), 9–21. <https://doi.org/10.1016/j.neuroimage.2012.10.034>
- [42] Linda Onnasch, Paul Schweidler, and Helena Schmidt. 2023. The potential of robot eyes as predictive cues in HRI—an eye-tracking study. *Frontiers in Robotics and AI* 10 (2023). <https://doi.org/10.3389/frobt.2023.1178433>
- [43] Peter S. Park. 2022. The Evolution of Cognitive Biases in Human Learning. *Journal of Theoretical Biology* 541 (2022), 111031. <https://doi.org/10.1016/j.jtbi.2022.111031> arXiv:<https://doi.org/10.1016/j.jtbi.2022.111031>
- [44] Sabine Pfeiffer. 2016. Robots, Industry 4.0 and Humans, or Why Assembly Work Is More than Routine Work. *Societies* 6, 2 (2016). <https://doi.org/10.3390/soc6020016>
- [45] Michael Plastow. 2012. ‘Theory of mind’ II: difficulties and critiques. *Australasian Psychiatry* 20, 4 (2012), 291–294. <https://doi.org/10.1177/1039856212449670> PMID: 22767933.
- [46] Preeti Ramaraj. 2021. Robots that Help Humans Build Better Mental Models of Robots. In *Companion of the 2021 ACM/IEEE International Conference on Human-Robot Interaction*. Association for Computing Machinery, New York, NY, USA, 595–597. <https://doi.org/10.1145/3434074.3446365>
- [47] Roger Ratcliff and Gail McKoon. 2008. The Diffusion Decision Model: Theory and Data for Two-Choice Decision Tasks. *Neural Computation* 20, 4 (Apr 2008), 873–922. <https://doi.org/10.1162/neco.2008.12-06-420>
- [48] R. A. Rescorla and A. R. Wagner. 1972. *A Theory of Pavlovian Conditioning: Variations in the Effectiveness of Reinforcement and Nonreinforcement*. Appleton-Century-Crofts, New York, 64–99.
- [49] Tessa Rusch, Saurabh Steixner-Kumar, Prashant Doshi, Michael Spezio, and Jan Gläscher. 2020. Theory of mind and decision science: Towards a typology of tasks and computational models. *Neuropsychologia* 146 (2020), 107488. <https://doi.org/10.1016/j.neuropsychologia.2020.107488>
- [50] Kazuki Sakai, Koh Mitsuda, Yuichiro Yoshikawa, Ryuichiro Higashinaka, Takashi Minato, and Hiroshi Ishiguro. 2024. Effects of Demonstrating Consensus Between Robots to Change User’s Opinion. *International Journal of Social Robotics* 16, 7 (2024), 1509–1521. <https://doi.org/10.1007/s12369-024-01151-z>
- [51] Brian Scassellati. 2002. Theory of Mind for a Humanoid Robot. *Autonomous Robots* 12, 1 (2002), 13–24. <https://doi.org/10.1023/A:1013298507114>
- [52] Kazuhiko Shinozawa, Futoshi Naya, Junji Yamato, and Kiyoshi Kogure. 2005. Differences in effect of robot and screen agent recommendations on human decision-making. *International Journal of Human-Computer Studies* 62, 2 (2005), 267–279. <https://doi.org/10.1016/j.ijhcs.2004.11.003>
- [53] Andrew Stewart, Ming Cao, Andrea Nedic, Damon Tomlin, and Naomi Leonard. 2012. Towards Human–Robot Teams: Model-Based Analysis of Human Decision Making in Two-Alternative Choice Tasks With Social Feedback. *Proc. IEEE* 100, 3 (2012), 751–775. <https://doi.org/10.1109/JPROC.2011.2173815>
- [54] Momchil S. Tomov, Eric Schulz, and Samuel J. Gershman. 2021. Multi-task reinforcement learning in humans. *Nature Human Behaviour* 5, 6 (2021), 764–773. <https://doi.org/10.1038/s41562-020-01035-y>
- [55] Vaibhav V. Unhelkar, Shen Li, and Julie A. Shah. 2020. Decision-Making for Bidirectional Communication in Sequential Human-Robot Collaborative Tasks. In *Proceedings of the 2020 ACM/IEEE International Conference on Human-Robot Interaction*. 329–341. <https://doi.org/10.1145/3319502.3374779>
- [56] A. Vakunov, C.-L. Chang, F. Zhang, G. Sung, M. Grundmann, and V. Bazarevsky. 2020. MediaPipe Hands: On-device Real-time Hand Tracking. Online. <https://mixedreality.cs.cornell.edu/workshop>
- [57] Wietse van Dijk, Saskia J. Baltrusch, Ezra Dessers, and Michiel P. de Looze. 2023. The effect of human autonomy and robot work pace on perceived workload in human-robot collaborative assembly work. *Frontiers in Robotics and AI* 10 (2023). <https://doi.org/10.3389/frobt.2023.1244656>
- [58] Samuele Vinanzi, Massimiliano Patacchiola, Antonio Chella, and Angelo Cangelosi. 2019. Would a robot trust you? Developmental robotics model of trust and theory of mind. *Philosophical Transactions of the Royal Society B: Biological Sciences* 374, 1771 (2019), 20180032. <https://doi.org/10.1098/rstb.2018.0032>
- [59] Katherine S. Welfare, Matthew R. Hallowell, Julie A. Shah, and Laurel D. Riek. 2019. Consider the Human Work Experience When Integrating Robotics in the Workplace. In *Proceedings of the 2019 14th ACM/IEEE International Conference on Human-Robot Interaction (HRI)*. 75–84. <https://doi.org/10.1109/HRI.2019.8673139>
- [60] Katherine J. Williams, Madeleine S. Yuh, and Neera Jain. 2023. A Computational Model of Coupled Human Trust and Self-confidence Dynamics. *Journal of Human-Robot Interaction* 12, 3, Article 39 (2023), 29 pages. <https://doi.org/10.1145/3594715>
- [61] Carol Young, Ningshi Yao, and Fumin Zhang. 2019. Avoiding Chatter in an Online Co-Learning Algorithm Predicting Human Intention. In *Proceedings of the 2019 IEEE 58th Conference on Decision and Control (CDC)*. 6504–6509. <https://doi.org/10.1109/CDC40024.2019.9030038>
- [62] Arkady Zgonnikov, David Abbink, and Gustav Markkula. 2024. Should I Stay or Should I Go? Cognitive Modeling of Left-Turn Gap Acceptance Decisions in Human Drivers. *Human Factors* 66, 5 (2024), 1399–1413. <https://doi.org/10.1177/00187208221144561> PMID: 36534014.

- [63] Qi Zhang, Lin Wang, and Xiaofan Wang. 2024. Dynamics of coupled implicit and explicit opinions. *Automatica* 167 (2024), 111694. <https://doi.org/10.1016/j.automatica.2024.111694>
- [64] Xuan Zhao, Corey Cusimano, and Bertram F. Malle. 2015. Do People Spontaneously Take a Robot's Visual Perspective?. In *Proceedings of the Tenth Annual ACM/IEEE International Conference on Human-Robot Interaction Extended Abstracts*. 133–134. <https://doi.org/10.1145/2701973.2702044>
- [65] Ariel Zylberberg, Daniel M. Wolpert, and Michael N. Shadlen. 2018. Counterfactual Reasoning Underlies the Learning of Priors in Decision Making. *Neuron* 99, 5 (2018), 1083–1097.e6. <https://doi.org/10.1016/j.neuron.2018.07.035> arXiv:<https://doi.org/10.1016/j.neuron.2018.07.035>
- [66] Şemsettin Çiğdem, Ieva Meidute-Kavaliauskiene, and Bülent Yıldız. 2023. Industry 4.0 and Industrial Robots: A Study from the Perspective of Manufacturing Company Employees. *Logistics* 7, 1 (2023). <https://doi.org/10.3390/logistics7010017>

Received XX September 2024; revised XX XXXXX 20XX; accepted XX XXXXX 20XX